Compositional heterogeneity and outgroup choice influence the internal phylogeny of the ants

Marek L. Borowiec*[a], Christian Rabeling[b], Seán G. Brady[c], Brian L. Fisher[d], Ted R. Schultz[c], and Philip S. Ward[a]

[a]Department of Entomology and Nematology, One Shields Avenue, University of California at Davis, Davis, California, 95616, USA
[b]School of Life Sciences, Social Insect Research Group, Arizona State University, Tempe, Arizona, 85287, USA
[c]Department of Entomology, National Museum of Natural History, Smithsonian Institution, Washington, D.C., USA
[d]Department of Entomology, California Academy of Sciences, San Francisco, California, 94118, USA

Abstract

Knowledge of the internal phylogeny and evolutionary history of ants (Formicidae), the world's most species-rich clade of eusocial organisms, has dramatically improved since the advent of molecular phylogenetics. A number of relationships at the subfamily level, however, remain uncertain. Key unresolved issues include placement of the root of the ant tree of life and the relationships among the so-called poneroid subfamilies. Here we assemble a new data set to attempt a resolution of these two problems and carry out divergence dating, focusing on the age of the root node of crown Formicidae. For the phylogenetic analyses we included data from 110 ant species, including the key species *Martialis heureka*. We focused taxon sampling on non-formicoid lineages of ants to gain insight about deep nodes in the ant phylogeny. For divergence dating we retained a subset of 62 extant taxa and 42 fossils in order to approximate diversified sampling in the context of the fossilized birth-death process. We sequenced 11 nuclear gene fragments for a total of ~7.5 kb and investigated the DNA sequence data for the presence of among-taxon compositional heterogeneity, a property known to mislead phylogenetic inference, and for its potential to affect the rooting of the ant phylogeny. We found sequences of the Leptanillinae and several outgroup taxa to be rich in adenine and thymine (51% average AT content) compared to the remaining ants (45% average). To investigate whether this heterogeneity could bias phylogenetic inference we performed outgroup removal experiments, analysis of compositionally homogeneous sites, and a simulation study. We

*Corresponding author.
Current address: School of Life Sciences, Social Insect Research Group, Arizona State University, Tempe, Arizona, 85287, USA.
E-mail address: petiolus@gmail.com (M. L. Borowiec).

found that compositional heterogeneity indeed appears to affect the placement of the root of the ant tree but has limited impact on more recent nodes. We put forward a novel hypothesis regarding the rooting of the ant phylogeny, in which *Martialis* and the Leptanillinae together constitute a clade that is sister to all other ants. After correcting for compositional heterogeneity this emerges as the best-supported hypothesis of relationships at deep nodes in the ant tree. The results of our divergence dating under the fossilized birth-death process and diversified sampling suggest that the crown Formicidae originated during the Albian or Aptian ages of the Lower Cretaceous (103–124 Ma). In addition, we found support for monophyletic poneroids comprising the subfamilies Agroecomyrmecinae, Amblyoponinae, Apomyrminae, Paraponerinae, Ponerinae, and Proceratiinae, and well-supported relationships among these subfamilies except for the placement of Proceratiinae and (Amblyoponinae + Apomyrminae). Our phylogeny also highlights the non-monophyly of several ant genera, including *Protanilla* and *Leptanilla* in the Leptanillinae, *Proceratium* in the Proceratiinae, and *Cryptopone*, *Euponera*, and *Mesoponera* within the Ponerinae.

Key words: Systematic bias, phylogenetics, systematics, diversified sampling, fossilized birth-death process

1. Introduction

Ants are among the world's dominant social insects, with more species and greater ecological impact than any other group of eusocial animals (Hölldobler and Wilson, 1990). Knowledge of ant phylogeny is vital to understanding the processes driving the evolution of these ubiquitous and diverse organisms.

About 90% of extant ant diversity, or almost 11,000 species and 9 of 16 subfamilies, belongs to a group dubbed the "formicoid clade" (Brady et al., 2006). The relationships among the subfamilies of the formicoid clade are well-resolved. This contrasts with the uncertain branching order of lineages outside of formicoids. Two enduring issues in higher ant phylogeny, highlighted by recent studies (Moreau et al., 2006; Brady et al., 2006; Rabeling et al., 2008) and a review by Ward (2014), include the identity and composition of the lineage that is sister to all other extant ants, and whether the so-called poneroid subfamilies (Agroecomyrmecinae, Amblyoponinae, Apomyrminae, Paraponerinae, Ponerinae, Proceratiinae) form a clade or a grade.

In molecular phylogenetic studies published to date, two ant subfamilies, the Martialinae and Leptanillinae (recently redefined to include the genus *Opamyrma*; Ward and Fisher (2016)), have been competing for the designation as the sister group to all other ants (Figure 1) (Rabeling et al., 2008; Kück et al., 2011; Moreau and Bell, 2013; Ward and Fisher, 2016). Rabeling et al. (2008) discovered and described *Martialis heureka*, and inferred that this sole species of the morphologically divergent Martialinae is the sister species to all other ants. Subsequent phylogenies, however, proposed that either the subfamily Leptanillinae is the lineage first branching from the rest of the ants (Kück et al., 2011), or were ambiguous about the placement of the ant root (Moreau and Bell, 2013).

The monophyly of the poneroid subfamilies was recovered by Moreau et al. (2006) but it was later contested by Brady et al. (2006) and Rabeling et al. (2008). Brady et al. (2006) pointed out that long-branch attraction may be responsible for poneroid monophyly and found that non-monophyly of poneroids could not be rejected based on their data set of seven nuclear gene fragments. Most subsequent phylogenetic studies failed to satisfactorily resolve this issue (reviewed in Ward (2014))

although poneroid monophyly was recovered with strong support by Ward and Fisher (2016). A recently published phylogenomic study also supported poneroid monophyly (Branstetter et al., 2017b). The phylogenomic data were apparently insufficient, however, to resolve relationships among poneroid lineages because of low taxon sampling (Branstetter et al., 2017b).

In addition to the phylogenetic uncertainty present in the above mentioned studies, there is also potential for systematic bias to preclude correct inference of ant relationships, especially near the root of the ant tree (Ward, 2014). This is because most ants are relatively guanine and cytosine- (GC) rich compared to many aculeate outgroups and species of the Leptanillinae, which are unusually adenine and thymine- (AT) rich. Such compositional heterogeneity is known to mislead phylogenetic inference (Jermiin et al., 2004) and most of the commonly used models of sequence evolution do not take it into account. This and other potential violations may lead to poor model fit, which was demonstrated in phylogenetics in general (Brown, 2014) and in an ant phylogeny specifically (Rabeling et al., 2008). It is thus possible that the basal position of the Leptanillinae appearing in some studies is an artifact resulting from model misspecification.

To address these issues of uncertainty and potential bias near the base of the ant tree of life, we assembled a new comprehensive data set that included all ant subfamilies, with sampling focused on non-formicoid lineages. The amount of sequence data we gathered is significantly greater than in previous studies that included the pivotal species *Martialis heureka*. We investigated the potential of these data to be biased by base-frequency heterogeneity and implemented strategies aimed at minimizing such bias.

Another outstanding question concerns the age of the most-recent common ancestor of ants, which has been variously estimated to have lived as recently as ca. 115 Ma (Brady et al., 2006) or as early as 168 Ma (Moreau et al., 2006), with the oldest undisputed crown formicid fossil *Kyromyrma neffi* dated at 92 Ma (Grimaldi and Agosti, 2000; Barden, 2017). Efforts to infer the age of origin of crown ants have been conducted thus far using either penalized likelihood (Sanderson, 2002) or node dating in a Bayesian framework (Drummond and Rambaut, 2007). Here we take advantage of the fossilized birth-death process framework (Heath et al., 2014), which was recently extended to accommodate diversified taxon sampling (Zhang et al., 2016).

The recently developed fossilized birth-death process (FBD) approach to divergence dating provides several advantages over the node-dating approach, as it explicitly treats both extant and fossil taxa as parts of the same underlying diversification process. This is different from the node-dating approach, where fossils only provide clues about the probability-density distributions of ages for certain splits (Heath et al., 2014). FBD is thus able to avoid some of the challenges documented for node-dating, such as formulation of the statistical problem accidentally precluding reasonable age estimate for a node of interest (Brown and Smith, 2017). Early implementations of the FBD, however, shared the assumption of other Bayesian divergence-time estimation methods that taxon sampling reflects complete or random sampling of the diversification process that created the phylogeny. Because phylogenies of higher taxa aim for maximizing phylogenetic diversity (Höhna et al., 2011), this assumption is often violated and is known to cause biased age estimates (Beaulieu et al., 2015). The most recent implementation of the FBD accounts for this by explicitly allowing modeling under a diversified sampling scheme (Zhang et al., 2016).

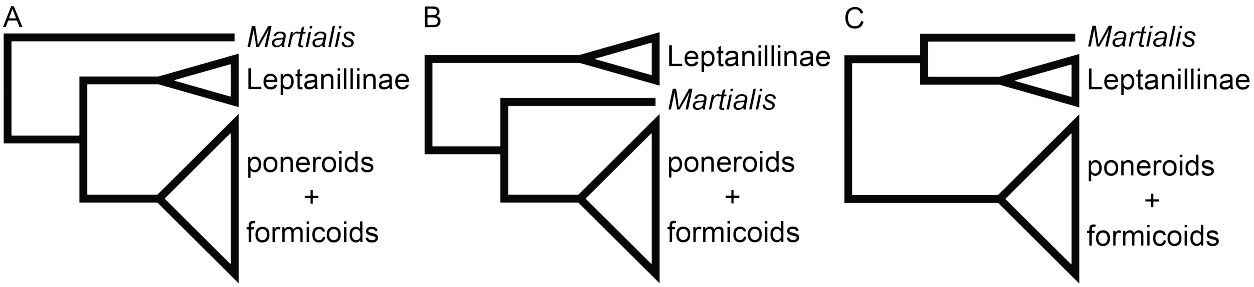

Figure 1: Comparison of alternative hypotheses for the root of the ant phylogeny. A, *Martialis* sister to all other ants (Rabeling et al., 2008); B, Leptanillinae sister to all other ants, including *Martialis* (Kück et al., 2011); C, *Martialis* plus Leptanillinae sister to all other ants (this study).

2. Methods

2.1. Taxon sampling and data collection

We collected data from 11 nuclear loci for 110 ant species, including *Martialis heureka*, and 13 outgroup taxa. Our data set has extensive sampling within Leptanillinae (21 species), all major lineages of the poneroids (66 species), and at least one representative of all formicoid subfamilies (22 species). The sequence data comes from *28S ribosomal DNA* (*28S*) and ten nuclear protein-coding genes: *abdominal-A* (*abdA*), *elongation factor 1-alpha F2 copy* (*EF1aF2*), *long wavelength rhodopsin* (*LW Rh*), *arginine kinase* (*argK*), *topoisomerase I* (*Top1*), *ultrabithorax* (*Ubx*), *DNA pol-delta* (*POLD1*), *NaK ATPase* (*NaK*), *antennapedia* (*Antp*), and *wingless* (*Wg*). Sequences were assembled with Sequencher v5.2.2 (Gene Codes Corporation, Ann Arbor, MI, U.S.A.), aligned with Clustal X v2.1 (Thompson et al., 1997), and manually edited and concatenated with MacClade v4.08 (Maddison and Maddison, 2005). We excluded introns, autapomorphic indels (9 bp *abdA*, 3 bp *EF1aF2*, 9 bp *Ubx*, 3 bp *POLD1*, 3 bp *NaK*, 75 bp *Antp*, 3 bp *Wg*), and hypervariable regions of *28S*. The resulting data matrix is 7,451 bp long and has no missing data except for gaps introduced by non-autapomorphic indels, which constitute 3% of the data. Our protocols for extraction and amplification were described in detail in Ward et al. (2010) and Ward and Fisher (2016). Of the 1,353 sequences, 676 were newly generated for this study (GenBank accessions XXXXXXXX-XXXXXXXX [submission in progress]; Supplementary Table 4).

2.2. Compositional heterogeneity

We assessed compositional heterogeneity using methods implemented in the p4 phylogenetics library (Foster, 2004). To investigate whether our data significantly departed from the assumption of homogeneity across taxa we applied two tests: 1) a χ^2 test for compositional heterogeneity, and 2) a more sensitive, simulation-based test corrected for phylogeny. The phylogeny-corrected tests involved inferring a neighbor-joining tree for the data, constructed with BioNJ (Gascuel, 1997), onto which we simulated 1,000 replicates using GTR+4Γ model. The distribution of sequence compositions in the empirical data were then compared against simulated data. Following the finding that the combined data set failed both the χ^2 and phylogenetically-corrected tests, we further divided the data set into partitions as follows: 1) each locus as its own partition, and 2) first, second, and third codon position within each locus assigned to separate partitions. We then ran the two compo-

sitional heterogeneity tests on each partition separately and recorded the results. We also computed base frequencies for each taxon and partition using AMAS (Borowiec, 2016).

2.3. *Data matrices*

In addition to the full data set, we composed two different matrices by excluding the most AT-rich and the most GC-rich outgroups, respectively. To this end, we first ranked non-ant taxa by AT content and then removed six taxa that had either the highest or lowest AT content, which also corresponded to above or below mean AT content for the entire data set. We retained moderately AT-rich *Pristocera* MG01 as the external outgroup.

We also constructed a data set from which we removed all heterogeneous partitions (i.e., *28S*, all third codon positions, and first codon positions of *POLD1* and *Ubx*).

Selected statistics of the four analyzed data matrices are in the first four rows of Table 1.

Table 1: Data properties.

Data matrix	Length	Percent gaps	Variable sites	Parsimony informative sites
Full data set	7451	3.0	3902	3369
AT-rich outgroups removed	7451	3.0	3806	3237
GC-rich outgroups removed	7451	3.0	3825	3291
Homogeneous partitions	3995	2.7	1181	831
28S	845	6.8	425	317
abdA	621	3.7	311	258
argK	673	0.3	334	296
Antp	865	14.0	497	397
EF1aF2	517	0.0	206	194
LW Rh	458	0.0	287	262
NaK	955	0.0	409	376
POLD1	583	0.0	374	325
Top1	880	0.0	477	426
Ubx	630	0.7	313	280
Wg	424	3.4	269	238
All 1st codon pos.	2200	2.5	829	620
All 2nd codon pos.	2199	2.5	536	349
All 3rd codon pos.	2207	2.5	2112	2083

2.4. *Partitioning*

In the light of recent criticism of the k-means partitioning strategy (Baca et al., 2017), for each of the four data sets we used two different strategies for partitioning: a 'greedy' algorithm on predefined user partitions and the k-means partitioning algorithm (Frandsen et al., 2015) as implemented in PartitionFinder 2 pre-release v13 (Lanfear et al., 2017). The greedy strategy relies on user-defined sets of characters as input and our predefined sets constituted sites from the three codon positions in each of the loci used, except for *28S* which was defined as a single set. We used a maximum-likelihood tree generated with the fast RAxML algorithm ("-f E" option) (Stamatakis, 2014) as

the starting tree for each PartitionFinder run, which then used PhyML for subsequent steps of the algorithm (Guindon et al., 2010). Because of our use of MrBayes in downstream analyses, we restricted models to be evaluated by PartitionFinder to those available in that program.

2.5. Phylogenetics

We constructed phylogenies for all empirical data sets using Bayesian inference with MrBayes v3.2.6 (Ronquist et al., 2012) and maximum-likelihood with IQ-TREE v1.4.2 beta (Nguyen et al., 2014). For the Bayesian analyses, we ran two separate runs, four chains each, for 20 to 80 million generations for each of the eight analyses. We used a 20% burnin fraction and determined mixing and convergence by examining output of MrBayes "sump" command, including average standard deviation of split frequencies (below < 0.01), effective sample size (ESS) for each parameter (minimum 200), and potential scale reduction factor (PSRF) near 1.0. In the maximum-likelihood analyses we specified the same partitioning schemes and substitution models as for the Bayesian inference. We changed the default IQ-TREE settings by using the slow nearest-neighbor interchange search ("-allnni" option) and setting the number of unsuccessful iterations to stop at 1,000 instead of the default 100 ("-numstop" option). We assessed support by running 2,000 ultrafast boostrap replicates (Minh et al., 2013). The authors of this fast bootstrap approximation point out that this algorithm tends to overestimate probability of a correct relationship under 70% support but is more unbiased than RAxML's rapid bootstrapping above that threshold, resulting in 95% support being approximately equal to 95% probability of a relationship being true under the true model. Therefore, support at or above 95% should be interpreted as significant (Minh et al., 2013). We also attempted analyses under tree-heterogeneous models implemented in p4 (Foster, 2004) and nhPhyloBayes (Blanquart and Lartillot, 2008) on the full data matrix, but these turned out to be prohibitively computationally expensive, requiring by our estimate a minimum of five months to reach convergence.

2.6. Simulation

To further assess the sensitivity of the ant phylogeny to bias we simulated a data set with compositional heterogeneity comparable to that present in our data set. In particular, we were interested in investigating whether the position of *Martialis* could be incorrectly inferred as sister to the poneroids plus formicoids clade even if the data were simulated on a topology where *Martialis* is sister to Leptanillinae. To create the simulated data set we first split our empirical alignment, excluding ribosomal *28S*, into alignments of first, second, and third codon positions. We then used a fixed topology which had *Martialis* as sister to Leptanillinae, in this case the Bayesian posterior consensus from the full data set analysis under k-means partitioning, to estimate branch lengths for each of the three alignments. To estimate the branch lengths we used IQ-TREE (Nguyen et al., 2015) under the general time-reversible model with rate heterogeneity described by a proportion of invariant sites and a gamma distribution discretized into four bins (GTR+pinv+4Γ). For each of the codon position alignments we also calculated the proportion of invariant sites and base frequencies for all taxa using AMAS (Borowiec, 2016). Furthermore, we calculated average base frequencies for alignments composed of first and second positions. For the third codon positions alignment we calculated two average base frequencies: one for the 25 most AT-rich taxa, represented almost exclusively by Leptanillinae species and some of the outgroups, and the other for

all remaining taxa, thus approximating mean base frequencies for AT-rich and GC-rich taxa, respectively. We then used the topologies with branch lengths, proportion of invariant sites, and empirical base frequencies to simulate three separate alignments, each 2,200 sites long, similar to the empirical data, under GTR+pinv+4Γ using p4 (Foster, 2004). For the alignments imitating first and second codon positions we simulated the data under a tree-homogeneous model, but for the third codon position alignment we used two composition vectors corresponding to the two empirical means of AT-rich (A: 0.24, C: 0.24, G: 0.23, T: 0.29) and GC-rich sequences (A: 0.16, C: 0.33, G: 0.31, T: 0.20) at that position. The AT-rich frequencies were applied to the Leptanillinae and outgroup taxa considered AT-rich in our outgroup taxa removal experiments outlined above. We replicated the simulation 100 times for each alignment under different starting seed numbers. We then performed maximum-likelihood analyses under GTR+pinv+4Γ (using IQ-TREE settings as described above) for the concatenated simulated data as well as each of the three simulated alignments separately. Following the inference we constructed majority-rule consensus trees using all 100 maximum-likelihood trees for all codon position simulations and the concatenated alignments in order to visualize the topology recovered from simulated alignments.

2.7. Divergence time estimation

We performed divergence dating under the fossilized birth-death process (Heath et al., 2014) and diversified sampling, as implemented in MrBayes v3.2.6 (Ronquist et al., 2012; Zhang et al., 2016). To obtain a taxon sample that most closely approximates diversified sampling *sensu* Höhna et al. (2011), i.e., one extant descendant sampled for each branch that was present at a given time in the past, we pruned our original alignment down to 62 species. To calibrate the analysis we used 42 fossil calibrations (See Supplementary Table 3) and a diffuse root node exponential prior with a mean of 250 Ma and offset at 150 Ma (just older than the oldest fossil calibration used). Because we did not include morphological data in our analysis to place the fossils ("total evidence" dating sensu Ronquist et al. (2012)), we assigned them to appropriate groups via monophyly constraints (Heath et al., 2014). For this analysis we also constrained the topology of outgroup taxa to correspond to the aculeate phylogeny recovered by a recent phylogenomic study (Branstetter et al., 2017a). We chose the topology from this study over that of Peters et al. (2017) because the latter did not include Rhopalosomatidae and Sierolomorphidae and thus arguably had insufficient taxon sampling to correctly place Vespidae.

We ran the analysis with four runs, each with six incrementally heated chains, for 100 million generations and discarded 10% of the samples as burn-in. The analysis was unpartitioned, with the GTR+6Γ substitution model and a relaxed independent clock model with rate drawn from a gamma distribution. We checked for convergence by examining the average standard deviation of split frequencies towards the end of the run (<0.006), potential scale reduction factor values for each parameter (maximum 1.028, average 1.001), and effective sample sizes (>500 for combined runs). We examined MCMC trace files with Tracer v1.5 to confirm that the two runs converged on all parameters and to compare posterior distributions to the analysis without data (i.e., under the prior).

2.8. *Data availability*

All data matrices, configurations for and output from PartitionFinder, Bayesian, and maximum-likelihood analyses, as well as custom scripts used are available the Zenodo data repository, DOI: 10.5281/zenodo.838799.

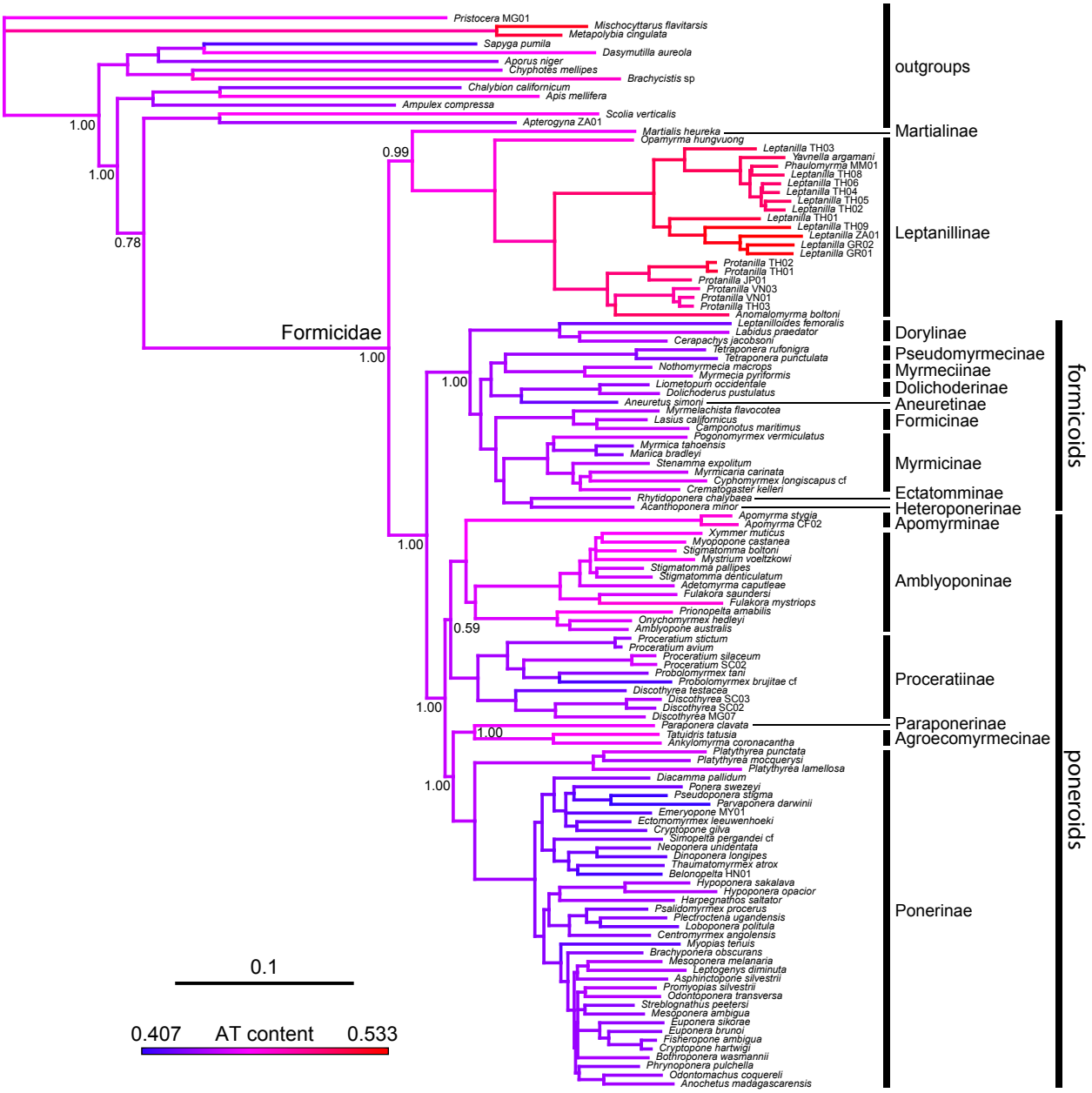

Figure 2: Preferred phylogenetic hypothesis for the ingroup (Formicidae), with AT content indicated for each terminal taxon. Tree topology with branch lengths from the Bayesian analysis of the full data matrix under k-means partitioning strategy. See Supplementary Figure 2 for support values on all nodes. Warmer branch colors signify higher AT content. Scale in expected substitutions per site.

3. Results

We first summarize results regarding compositional heterogeneity, followed by a discussion of the placement of the formicid root as it was impacted by the different methods. Second, we present phylogenetic findings which were less sensitive to different analytical treatments, including poneroid monophyly, the relationships within poneroids, and non-monophyly of some of the non-formicoid genera.

3.1. Compositional heterogeneity

Within the ingroup, ants in the Leptanillinae stands out as particularly AT-rich at 50.9% on average compared to a mean of 46.2% for all taxa (or 44.9% for non-leptanilline ants). At 46.6%, *Martialis* is close to the mean (Figure 2, Supplementary Table 1).

We found considerable compositional heterogeneity among taxa in our data set, mostly confined to third codon positions. Overall difference in AT content among taxa was 12.6% across the entire data set. This difference was equal to 37.3% at third codon positions, compared to only 3.5% at first codon positions and 1.1% at the second codon positions. Third codon positions also accounted for 56.7% variable sites and 61.8% parsimony informative sites of the data set.

Consistent with this pattern, the phylogeny-corrected test identified all third codon partitions as those for which the homogeneity assumption could be rejected with a $p < 0.05$ (Supplementary Table 2). In addition to the third codon positions, *28S*, and first codon positions of *POLD1* and *Ubx* were found to violate the homogeneity assumption using this test. Similar to the phylogeny-corrected test, the χ^2 test identified all of the third codon positions as heterogeneous but it did not reject the homogeneity assumption for *28S* and first codon positions of *POLD1* and *Ubx* (Supplementary Table 2).

Compositional heterogeneity was also high among the outgroups. Those that fell above the mean AT content for the entire alignment included (in order of decreasing AT content) *Mischocyttarus flavitarsis*, *Metapolybia cingulata*, *Brachycistis* sp., *Apis mellifera*, *Dasymutilla aureola*, *Scolia verticalis*, and *Pristocera* MG01. The outgroup species that were more GC-rich than average were (in order of decreasing AT content) *Chyphotes mellipes*, *Ampulex compressa*, *Apterogyna* ZA01, *Aporus niger*, *Chalybion californicum*, and *Sapyga pumila* (Supplementary Table 1).

3.2. Analyses of the full data matrix

With all taxa retained and no attempt at reducing the compositional heterogeneity of the data, the partitioning strategy has a strong effect on the results. Under the k-means strategy *Martialis heureka* is sister to the Leptanillinae with strong support of $pp = 0.99$ in the Bayesian analysis (Figure 2; Supplementary Figure 2) and low support of 87% bootstrap in the maximum-likelihood tree (Supplementary Figure 4). Under the greedy analyses, both Bayesian and maximum-likelihood trees recover a topology where the Leptanillinae are sister to the remaining Formicidae including *Martialis*, although support for this topology is below significance ($pp = 0.81$ and bootstrap 93%; Supplementary Figures 1 and 3).

3.3. *Effects of outgroup removal*

Relative to the full data matrix with all 13 outgroup species, removal of the AT-rich outgroups (*Apis mellifera*, *Brachycistis* sp., *Dasymutilla aureola*, *Scolia verticalis*, *Metapolybia cingulata*, and *Mischocyttarus flavitarsis*) shifts support towards a tree where *Martialis* and the Leptanillinae together form a clade that is sister to all other ants. In consensus Bayesian trees, the support for this clade is at $pp = 0.91$ under greedy (Supplementary Figure 5) and $pp = 1.0$ under the k-means partitioning strategy (Supplementary Figure 6). Under maximum-likelihood, the effect is less obvious, as the ML tree under greedy partitioning has *Martialis* sister to formicoids and poneroids but now with only 50% bootstrap support (Supplementary Figure 7). In the k-means maximum-likelihood tree, *Martialis* and Leptanillinae form a clade supported in 99% bootstrap replicates (Supplementary Figure 8).

Removal of GC-rich outgroups (*Ampulex compressa*, *Aporus niger*, *Apterogyna* ZA01, *Chalybion californicum*, and *Chyphotes mellipes*) reinforces support for the topology where Leptanillinae are sister to *Martialis* plus formicoids plus poneroids with $pp = 1.0$ under greedy partitioning (Supplementary Figure 9) and $pp = 0.98$ under k-means in Bayesian analyses (Supplementary Figure 10). The same pattern is present in maximum-likelihood trees, which both show Leptanillinae sister to *Martialis* plus formicoids and poneroids. Under greedy analyses bootstrap support for this clade is 99% (Supplementary Figure 11) and under k-means it is 96% (Supplementary Figure 12).

3.4. *Compositionally homogeneous matrix*

The analyses of homogeneous data partitions result in a tree where *Martialis* is sister to the Leptanillinae with strong support regardless of partitioning scheme and inference method (Table 2). Bayesian trees under both greedy and k-means partitioning strategies show $pp = 1.00$ (Supplementary Figures 13 and 14). Under maximum-likelihood this node is supported in 100% bootstrap replicates under both greedy k-means partitioning strategies (Supplementary Figures 15 and 16).

3.5. *Simulation*

In the maximum-likelihood analyses of simulated alignments imitating first codon positions the *Martialis* plus Leptanillinae clade, i.e., the topology under which the data were simulated, is recovered consistently (Supplementary Figure 17). For the alignments imitating second codon positions *Martialis* emerges as sister to the Leptanillinae in 96 out of 100 trees Supplementary Figure 18), and in the tree derived from the matrix imitating third codon positions *Martialis* is sister to the Leptanillinae in only 64 trees out of 100 (Supplementary Figure 19). The remaining 36 trees show *Martialis* either as sister to the poneroid plus formicoid clade, with Leptanillinae being sister to all other ants, or, alternatively as the sister group to all ants. The combined data set supports the *Martialis* plus Leptanillinae clade in 99 out of 100 trees (Supplementary Figure 20).

3.6. *Relationships among poneroid subfamillies*

The so-called poneroid ant subfamillies that include Agroecomyrmecinae, Amblyoponinae, Apomyrminae, Paraponerinae, Ponerinae, and Proceratiinae form a well supported clade. This result appears more robust to different analytics than the placement of the root of the tree. Support for this clade is often maximum in Bayesian analyses and generally above 90% bootstrap proportion in the

maximum-likelihood analyses, except for the data set with GC-rich outgroups removed, where the support is only 75% (Table 2).

Within the poneroid clade, another set of relationships that is well-supported across the analyses is the sister relationship of Agroecomyrmecinae and Paraponerinae, which is significantly supported in all analyses except in the maximum-likelihood trees inferred from the homogeneous data matrix. This clade is in turn sister to the Ponerinae in all analyses, although support varies. This relationship receives maximum support in all Bayesian analyses except for the data matrix with GC-rich outgroups removed. In maximum-likelihood trees support varies between 74% and 97% bootstrap replicates (Table 2).

The most problematic is placement of Proceratiinae and (Amblyoponinae + Apomyrminae), which in some analyses form a clade, and in others form a grade where Amblyoponinae plus Apomyrminae are the sister clade to all other poneroids and Proceratiinae is sister to the remaining subfamilies. The support for both of these alternatives is never significant, however (Table 2).

3.7. Non-monophyly of currently recognized genera

Several shallow nodes, well-supported regardless of the data set and analysis method, highlight non-monophyly of genera outside of the formicoid clade (Figure 2; Supplementary Figures 1–16).

In the Leptanillinae, the morphologically derived genus *Anomalomyrma* is nested within *Protanilla*, and two genera known only from males, *Phaulomyrma* and *Yavnella*, are nested within *Leptanilla*.

Within the small subfamily Proceratiinae, the four species of *Proceratium* included in our data matrices were paraphyletic with respect to *Probolomyrmex*.

Under all analyses we recover three non-monophyletic genera within Ponerinae: *Cryptopone gilva* and *Cryptopone hartwigi* included here are only very distantly related, the genus *Euponera* is paraphyletic with respect to the *Cryptopone hartwigi* plus *Fisheropone* clade, and *Mesoponera* is polyphyletic, here represented by *M. melanaria*, which is sister to *Leptogenys*, and *M. ambigua*, here sister to *Streblognathus peetersi*.

3.8. Divergence time analyses

Our divergence time analysis recovers a relatively young age for the most common ancestor of crown-group ants, estimated to have lived during the Albian or Aptian ages of the Lower Cretaceous (Figure 3, Table 3; median age 112 Ma, 95% highest posterior density interval 103–123 Ma). The crown formicoids are estimated to have arisen ~101 Ma, closely followed by the split of *Martialis* from the Leptanillinae around 99 Ma, and the origin of poneroids at 92 Ma. The median ages inferred for the subfamilies where our taxon sampling spanned the root node are as follows: 45 for Agroecomyrmecinae, 75 Ma for Ambyloponinae plus Apomyrminae, 55 Ma for Dolichoderinae, 60 Ma for Formicinae, 66 Ma for Leptanillinae, 45 Ma for Myrmeciinae, 61 Ma for Myrmicinae, 73 Ma for Ponerinae, and 65 Ma for Proceratiinae.

4. Discussion

4.1. Compositional heterogeneity and the rooting of the ant tree

Earlier studies recognized the difficulty in rooting the ant tree of life (Brady et al., 2006; Rabeling et al., 2008) and our analyses confirm the supposition (Ward, 2014) that the effects of composi-

Table 2: Support for selected relationships in Bayesian consensus and maximum-likelihood (ML) trees. Support for Bayesian analyses is expressed in posterior probabilities rounded to two decimal places and for ML in percentage of bootstrap replicates. Ag: Agroecomyrmecinae, Am: Amblyoponinae plus Apomyrminae, for: formicoids, Le: Leptanillinae, Ma: Martialinae, Pa: Paraponerinae, Po: Ponerinae, pon: poneroids, Pr: Proceratiinae. NA signifies a case where the relationship was not recovered in the consensus or maximum-likelihood tree.

Matrix	Method	Partitioning	Ma + Le	Ma + (for + pon)	pon monophyl.	Ag + Pa	Po + (Ag + Pa)	Pr + Am	Pr + (Ag/Pa/Po)	Am + (Ag/Pa/Po)
Full	ML	greedy	NA	93	100	100	97	NA	77	NA
Full	ML	k-means	87	NA	92	98	88	71	NA	NA
Full	Bayes	greedy	NA	0.81	1.00	1.00	1.00	NA	0.54	NA
Full	Bayes	k-means	0.99	NA	1.00	1.00	1.00	0.59	NA	NA
AT-rich outgr. removed	ML	greedy	NA	50	99	100	92	NA	70	NA
AT-rich outgr. removed	ML	k-means	99	NA	97	99	83	64	NA	NA
AT-rich outgr. removed	Bayes	greedy	0.91	NA	1.00	1.00	1.00	0.5	NA	NA
AT-rich outgr. removed	Bayes	k-means	1.00	NA	1.00	1.00	1.00	0.64	NA	NA
GC-rich outgr. removed	ML	greedy	NA	99	99	100	95	NA	86	NA
GC-rich outgr. removed	ML	k-means	NA	96	75	96	73	NA	45	NA
GC-rich outgr. removed	Bayes	greedy	NA	1.00	1.00	1.00	1.00	NA	0.87	NA
GC-rich outgr. removed	Bayes	k-means	NA	0.98	0.88	0.99	0.88	NA	0.54	NA
Homogeneous	ML	greedy	100	NA	98	81	99	NA	NA	79
Homogeneous	ML	k-means	100	NA	98	78	100	NA	NA	72
Homogeneous	Bayes	greedy	1.00	NA	1.00	0.99	1.00	NA	NA	0.67
Homogeneous	Bayes	k-means	1.00	NA	1.00	0.93	1.00	0.50	0.50	NA

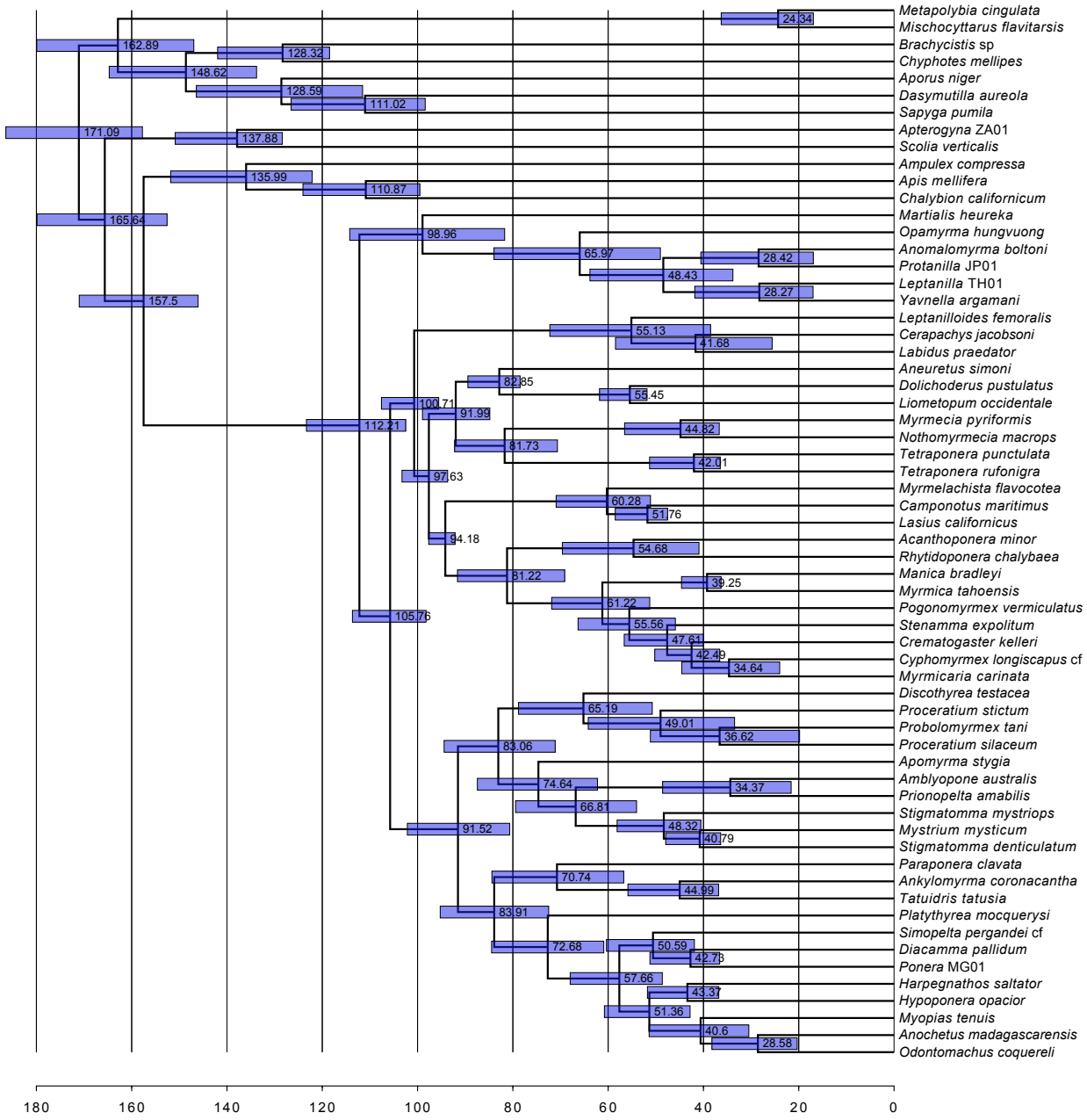

Figure 3: Chronogram from the divergence dating analysis under the fossilized birth-death process with diversified sampling, in MrBayes. Scale is in Ma. Bars depict the 95% highest posterior probability density of each estimate.

tional heterogeneity play a role. The outgroup removal experiments, exclusion of compositionally heterogeneous sites, and simulations all suggest that with greater compositional heterogeneity in the data the abnormally AT-rich Leptanillinae species are drawn more strongly to the base of the ant tree. As a result of this, the more GC-rich *Martialis* can erroneously cluster with the clade of formicoids and poneroids, as in Kück et al. (2011). When compositional heterogeneity is accounted for, as in the homogeneous data matrix, the Leptanillinae and *Martialis* emerge as sister taxa forming a strongly supported clade that is sister to all other ants.

Table 3: Comparison of divergence time estimates. Numbers for this study refer to median node age (95% highest posterior density) in Ma. Numbers from other studies are ranges of means/medians from across all analyses presented.

Crown taxon	This study	Brady et al. 2006	Moreau et al. 2006	Moreau and Bell 2013	Schmidt 2013
Formicidae	112 (103–123)	111–137	141–169	139–158	116–141
Leptanillinae (excl. *Opamyrma*)	48 (34–64)	68–89	102–123	72–104	NA
Amblyoponinae + Apomyrminae	75 (62–87)	92–118	113–143	NA	85–100
Proceratiinae	65 (51–79)	78–98	111–132	NA	74–88
Ponerinae	73 (61–84)	79–103	111–132	56–60	85–102
Dolichoderinae	55 (52–62)	71–76	86–97	53–66	NA
Myrmeciinae	45 (37–57)	46–52	NA	NA	NA
Formicinae	60 (51–71)	77–82	92–104	75–90	65–70
Myrmicinae	61 (51–72)	82–89	100–114	78–90	73–76
Dorylinae	>= 55 (39–72)	76–87	99–117	78–95	78–88

The selective outgroup removal experiment shows a trend in which support for the AT-rich Leptanillinae as sister to all other ants including *Martialis* is the strongest when only AT-rich outgroups are retained, moderate or weak when all outgroups (those that are AT- and GC-rich) are retained, and the weakest when all the AT-rich outgroups are removed. This suggests that the AT content of outgroup taxa indeed causes attraction of the above-average AT-rich Leptanillinae to the base of the ant tree. This finding has interesting implications for outgroup choice in phylogenetics in general, as it suggests that choice of outgroups should be made not only on the basis of their close relationship to the ingroup taxa, but also taking into account sequence divergence and other properties relative to the ingroup (Takezaki and Nishihara, 2016)

Finally, our simulations show that compositional heterogeneity similar to that in our empirical data matrix has the potential to cause bias resulting in the incorrect placement of Leptanillinae as sister to *Martialis* plus poneroids plus formicoids. The matrix designed to imitate third codon positions was simulated on a tree where *Martialis* was sister to Leptanillinae, but the maximum-likelihood trees inferred from this alignment often recover *Martialis* sister to all other ants or sister to the poneroids plus formicoids, both topologies recovered in previous studies (Rabeling et al., 2008; Kück et al., 2011). The tree topology used for the simulation is correctly recovered from the alignments imitating first and second codon positions in most cases. These alignments were simulated with base frequencies drawn from our empirical alignment and under a tree-homogeneous model. On a combined simulated data set the negative effect of sites emulating third codon positions is overwhelmed by the homogeneous data and the inferred tree is consistent with the topology on which the data were simulated in 99 out of 100 maximum-likelihood trees obtained from the simulated concatenated data. These effects appear not to be as strong as seen in our empirical data, but the simulation is a simplistic scenario that is likely to involve fewer confounding factors. In particular, 1) the same substitution model that generated the data could be used for inference (minus compositional heterogeneity), 2) the simulations attempted to capture only one dimension of the process heterogeneity, and 3) in our empirical data matrix compositionally heterogeneous sites were actually over-represented compared to the simulated matrix because of the heterogeneous *28S* partition, which was not taken into account when simulating the matrix imitating the non-homogenous third codon positions. The results from simulations imitating compositionally heterogeneous third codon position data demonstrate that compositional heterogeneity, at least in principle, has the potential to impact the position of *Martialis*.

If our interpretation of these results is correct, the species-poor clade of blind and subterranean Martialinae and Leptanillinae is the sister group to the remaining 99.5% species of the Formicidae. As pointed out before (Brady et al., 2006; Rabeling et al., 2008; Pie and Feitosa, 2015), this does not necessarily mean that the most-recent common ancestor of the ants was blind and lived underground (Lucky et al., 2013). Rather, this fact may reflect lower relative extinction rates experienced by these ants, perhaps due to the long-term stability of their subterranean environments, or different relative probabilities of evolutionary transitions between subterranean and epigaeic habits.

4.2. Relationships of poneroid subfamillies

In addition to further insight into the placement of the root of the ant phylogeny, we find evidence for poneroid monophyly. The question of poneroid monophyly vs. paraphyly was the second outstanding issue in higher ant phylogeny highlighted in a recent review (Ward, 2014). All our empirical analyses suggest poneroid monophyly, and in most instances this clade receives significant support, with the notable exception of analyses of the data matrix from which GC-rich outgroups were removed, i.e., where the phylogeny was potentially more susceptible to bias. Poneroid monophyly was first recovered in Moreau et al. (2006) but this result was questioned as doubtful by Brady et al. (2006), who emphasized contradictory results from their Bayesian and maximum-likelihood analyses of which the former supported monophyletic poneroids but the latter did not. Brady et al. (2006) also conducted ingroup-only analyses which supported topologies where no possible rooting could result in poneroid monophyly. Although we did not perform ingroup-only analyses here, taking into account more comprehensive taxon sampling, the higher amount of sequence data, and insensitivity of poneroid monophyly to the different data treatments, we interpret the support for the poneroid clade as strong. Poneroid monophyly has also been recovered in other phylogenetic studies of ants, including Moreau et al. (2006), some analyses of Brady et al. (2006), Ward and Fisher (2016), and a phylogenomic study (Branstetter et al., 2017b).

Similarly strongly-supported results involve the relationships among the poneroid clade subfamilies Agroecomyrmecinae, Paraponerinae, and Ponerinae. Although very disparate morphologically, Agroecomyrmecinae emerge as sister to Paraponerinae with significant support in all analyses, and this clade is in turn sister to the Ponerinae.

Our data are inconclusive on the relative position of Proceratiinae and (Amblyoponinae plus Apomyrminae), which sometimes emerge as a clade and at other times as a grade relative to the clade composed of Agroecomyrmecinae, Paraponerinae, and Ponerinae. If other results presented here are confirmed, the placement of (Ambyloponinae plus Apomyrminae) and Proceratiinae within the poneroid group would remain the last unsolved subfamily-level relationship in ants.

4.3. Non-monophyly of currently recognized genera

Our analyses recover several of the currently recognized ant genera as para- or polyphyletic. Although we do not favor inclusion of non-monophyletic groups in a classification, here we are only highlighting existing problems without proposing any formal taxonomic changes. We feel that proposing satisfactory resolutions requires additional research, as explained for each case below.

Among the Leptanillinae, we find the morphologically derived genus *Anomalomyrma* nested within samples identified by us as *Protanilla*. A more comprehensive evaluation of *Protanilla*-like leptanillines, including both males and workers, should be carried out for a better understanding

of diversity within the group. We find two other leptanilline genera, *Phaulomyrma* and *Yavnella*, nested within *Leptanilla*. Both these genera were described based on males not associated with workers (Wheeler and Wheeler, 1930; Kugler, 1987). Because the characters defining and differentiating leptanilline lineages based on males are not well understood (Ogata et al., 1995) and all of our *Leptanilla* specimens were males, we feel it would be premature to propose taxonomic changes. A critical reappraisal of leptanilline taxonomy using both morphology and molecular phylogenetics is clearly needed.

Our analyses find the proceratiine genus *Probolomyrmex* nested within the larger genus *Proceratium*. Several species currently in *Proceratium* were classified in the erstwhile genus *Sysphingta*. The differentiation between the two taxa was mostly based on the structure of the clypeus and shape of the petiole. Based on these characters, two of the *Proceratium* species included in our phylogeny, *P. avium* and *P. stictum*, would fit the old concept of *Sysphingta*, while the two other, *Proceratium silaceum* and *Proceratium* SC02, match *Proceratium* sensu stricto (*P. silaceum* is the type species of the genus). Previous authors (Brown, 1958; Urbani and Andrade, 2003), however, showed that considerable variation exists with regard to the characters originally used to distinguish *Proceratium* from *Sysphingta*. *Proceratium* taxonomy would thus benefit from a focused study and a re-evaluation of morphology under a modern phylogenetic framework.

Despite recent comprehensive taxonomic and phylogenetic work focusing on the Ponerinae (Schmidt, 2013; Schmidt and Shattuck, 2014), our analyses reveal three non-monophyletic genera within the subfamily.

Cryptopone is a case of a polyphyletic genus. The two species included here, *C. gilva* and *C. hartwigi*, are only very distantly related. The former is a part of the *Ponera* genus-group and the latter sister to *Fisheropone* and a part of the *Odontomachus* genus-group, as defined by Schmidt (2013). As noted by Schmidt and Shattuck (2014), the resolution of *Cryptopone* taxonomy would require a more thorough revision and sampling of all species attributed to this genus. Notably, our phylogeny did not include any species placed in the erstwhile genus *Wadeura*, which may well turn out to be yet another lineage unrelated to the type species *C. testacea*.

Euponera, which was recognized to form two morphologically distinct species groups by Schmidt and Shattuck (2014), is represented by *E. brunoi* and *E. sikorae* in our data set. In our phylogeny, *E. brunoi* is more closely related to "*Cryptopone*" *hartwigi* and *Fisheropone* than *E. sikorae*. Together, the paraphyletic *Euponera*, the species "*Cryptopone*" *hartwigi*, and *Fisheropone ambigua* form a well-supported group with well-resolved internal relationships. *Euponera* is divisible into two groups based on morphology but there are several species that cannot be placed with certainty even within the genus as presently defined (Schmidt and Shattuck, 2014). Assignment of *Euponera* species into two different genera should thus be postponed until more evidence is available.

Mesoponera, also found to be polyphyletic in our analyses, presents a particularly taxonomically challenging genus that would require a more comprehensive reexamination of morphology and inclusion of more species in a phylogeny for satisfactory resolution. See Schmidt and Shattuck (2014) for a more thorough discussion.

4.4. The age of extant ants

Our divergence-time analysis indicates that the most recent common ancestor of living ants originated during the Lower Cretaceous (103–124 Ma; median 113 Ma), an age estimate considerably younger than those obtained by some other recent studies. Moreau et al. (2006) concluded that ants

most likely arose 140–169 Ma while Moreau and Bell (2013) arrived at an estimate of 139–158 Ma. In contrast, Brady et al. (2006) proposed a younger age for the crown ants, 116–133 Ma.

Our study parallels the pattern for age estimates of the order Hymenoptera, which has often been inferred to be much older than the oldest hymenopteran fossils (Ronquist et al., 2012; Peters et al., 2017), but under fossilized birth-death process with diversified sampling its estimated age fell to within 20 Ma from the oldest known fossils (Zhang et al., 2016). In our study, the median age for the crown Formicidae, at 113 Ma, is also about 20 Ma older than the oldest undisputed crown-group fossils (Grimaldi and Agosti, 2000; Barden, 2017).

The ages we recovered for ant subfamilies where either few old crown-group fossils are known or only a few taxa were sampled are almost certainly underestimated (e.g. Dolichoderinae at 55 Ma, cf. Ward et al. (2010); Formicinae at 60 Ma, cf. Blaimer et al. (2015)). Future studies including more genus-level sampling of extant and extinct taxa are likely to modify these estimates in the direction of older dates.

5. Concluding remarks

Although more sequence data have often been shown to help resolve difficult phylogenetic questions, our study of ant phylogeny shows that systematic bias not accounted for by the commonly used tree-homogeneous models may adversely affect phylogenetic inference. Simply increasing the amount of data can in fact be detrimental if added sequences have properties that violate model assumptions (Huelsenbeck and Hillis, 1993), such as the substantial among-taxon compositional heterogeneity present in third codon positions and ribosomal 28S in our data set. The ideal solution to this problem would be use of substitution models that take into account process heterogeneity across the tree. Such models have been proposed (Foster, 2004; Blanquart and Lartillot, 2008; Jayaswal et al., 2014), but unfortunately their current implementations do not scale well for larger data sets, even for the modest amount of data present in our alignment. Alternatively, one can assess model adequacy through simulation-based tests of compositional heterogeneity (Foster, 2004), as in the current study.

The phylogenetic hypothesis presented here for deep nodes of the ant tree of life will soon be tested with genomic-scale data. Recent advances in sequencing and analysis has already produced data matrices with hundreds or even thousands of loci (Faircloth et al., 2014; Blaimer et al., 2015; Branstetter et al., 2017b). As the amount of available sequence data increases, it is important that the potential for model violation is carefully evaluated, as large data sets will likely be less prone to uncertainty but instead may give strongly-supported results that are wrong instead (Philippe and Roure, 2011). Tests of compositional heterogeneity, posterior predictive approaches to assessing model fit (Bollback, 2002; Brown and ElDabaje, 2008; Doyle et al., 2015), or sensitivity of results to removal of sites likely to introduce bias (Goremykin et al., 2015) should become a part of the standard phylogenomics toolkit.

Our understanding of the timeline of ant evolution will also likely benefit from more biologically realistic models resulting from recent developments in divergence-dating, such as placement of fossils using explicit information about morphology (Ronquist et al., 2012; Zhang et al., 2016), and from inclusion of more sequence data as well as more comprehensive taxon sampling.

6. Acknowledgements

For providing specimens used in this study we are grateful to Bob Anderson, Himender Bharti, Lech Borowiec, Bui Tuan Viet, Jim Carpenter, Katsuyuki Eguchi, Juergen Gadau, Dave General, Benoit Guénard, Nihara Gunawardene, Peter Hawkes, Armin Ionesco-Hirsch, Bob Johnson, Yeo Kolo, John LaPolla, John Lattke, Jack Longino, Randy Morgan, Michael Ohl, Christian Peeters, James Pitts, Julian Resasco, Keve Ribardo, Riitta Savolainen, Chris Schmidt, Justin Schmidt, Mike Sharkey, Andy Suarez, Simon van Noort, and Masashi Yoshimura. This research was supported by U.S. National Science Foundation grants EF-0431330, DEB-1402432, DEB-0842204, DEB-1354996, DEB-1456964, and DEB-1654829.

References

Andrade, M. L. D. (1994). Fossil Odontomachiti ants from the Dominican Republic (Amber Collection Stuttgart: Hymenoptera, Formicidae. VII: Odontomachiti). *Stuttg. Beitr. Naturkd. Ser. B (Geol. Paläontol.)*, 199:1–28.

Antropov, A. V. (2000). Digger wasps (Hymenoptera, Sphecidae) in Burmese amber. *Bull. Nat. Hist. Mus. Geol. Ser.*, 56(1):59–77.

Antropov, A. V. (2011). A new tribe of fossil digger wasps (Hymenoptera: Crabronidae) from the Upper Cretaceous New Jersey amber and its place in the subfamily Pemphredoninae. *Russ. Entomol. J.*, 20(3):229–240.

Archibald, S. B., Cover, S. P., and Moreau, C. S. (2006). Bulldog ants of the Eocene Okanagan Highlands and history of the subfamily (Hymenoptera: Formicidae: Myrmeciinae). *Ann. Entomol. Soc. Am.*, 99(3):487–523.

Aria, C., Perrichot, V., and Nel, A. (2011). Fossil Ponerinae (Hymenoptera: Formicidae) in Early Eocene amber of France. *Zootaxa*, 2870:53–62.

Baca, S. M., Toussaint, E. F., Miller, K. B., and Short, A. E. (2017). Molecular phylogeny of the aquatic beetle family Noteridae (Coleoptera: Adephaga) with an emphasis on data partitioning strategies. *Mol. Phylogenet. Evol.*, 107:282–292.

Barden, P. (2017). Fossil ants (Hymenoptera: Formicidae): ancient diversity and the rise of modern lineages. *Myrmecol. News*, 24:1–30.

Barden, P. and Grimaldi, D. A. (2016). Adaptive radiation in socially advanced stem-group ants from the Cretaceous. *Curr. Biol.*, 26(4):515–521.

Baroni Urbani, C. (2000). Rediscovery of the Baltic amber ant genus *Prionomyrmex* (Hymenoptera, Formicidae) and its taxonomic consequences. *Eclogae Geol. Helv.*, 93:471–480.

Beaulieu, J. M., O'Meara, B. C., Crane, P., and Donoghue, M. J. (2015). Heterogeneous rates of molecular evolution and diversification could explain the Triassic age estimate for angiosperms. *Syst. Biol.*, 64(5):869–878.

Bennett, D. J. and Engel, M. S. (2005). A primitive sapygid wasp in Burmese amber (Hymenoptera: Sapygidae). *Acta Zool. Cracoviensia*, 48(3-1):1–9.

Blaimer, B. B., Brady, S. G., Schultz, T. R., Lloyd, M. W., Fisher, B. L., and Ward, P. S. (2015). Phylogenomic methods outperform traditional multi-locus approaches in resolving deep evolutionary history: a case study of formicine ants. *BMC Evol. Biol.*, 15(1):e271.

Blanquart, S. and Lartillot, N. (2008). A site- and time-heterogeneous model of amino acid replacement. *Mol. Biol. Evol.*, 25(5):842–858.

Bollback, J. P. (2002). Bayesian model adequacy and choice in phylogenetics. *Mol. Biol. Evol.*, 19(7):1171–1180.

Borowiec, M. L. (2016). AMAS: a fast tool for alignment manipulation and computing of summary statistics. *PeerJ*, 4:e1660.

Boudinot, B. E., Probst, R. S., Brandão, C. R. F., Feitosa, R. M., and Ward, P. S. (2016). Out of the Neotropics: newly discovered relictual species sheds light on the biogeographical history of spider ants (*Leptomyrmex*, Dolichoderinae, Formicidae). *Syst. Entomol.*, 41(3):658–671.

Brady, S. G., Fisher, B. L., Schultz, T. R., and Ward, P. S. (2014). The rise of army ants and their relatives: diversification of specialized predatory doryline ants. *BMC Evol. Biol.*, 14(1):93.

Brady, S. G., Schultz, T. R., Fisher, B. L., and Ward, P. S. (2006). Evaluating alternative hypotheses for the early evolution and diversification of ants. *Proc. Natl. Acad. Sci. U.S.A.*, 103:18172–18177.

Branstetter, M. G., Danforth, B. N., Pitts, J. P., Faircloth, B. C., Ward, P. S., Buffington, M. L., Gates, M. W., Kula, R. R., and Brady, S. G. (2017a). Phylogenomic insights into the evolution of stinging wasps and the origins of ants and bees. *Curr. Biol.*, 27(7):1019–1025.

Branstetter, M. G., Longino, J. T., Ward, P. S., and Faircloth, B. C. (2017b). Enriching the ant tree of life: enhanced UCE bait set for genome-scale phylogenetics of ants and other Hymenoptera. *Methods Ecol. Evol.*, 9:768–776.

Brothers, D. J. (1974). The first recent species of *Protomutilla* (Hymenoptera: Mutillidae; Myrmosinae). *Psyche (Cambridge)*, 81(2):268–271.

Brown, W. L., J. (1958). Contributions toward a reclassification of the Formicidae. II. Tribe Ectatommini (Hymenoptera). *Bull. Mus. Comp. Zool.*, 118:173–362.

Brown, J. M. (2014). Predictive approaches to assessing the fit of evolutionary models. *Syst. Biol.*, 63(3):289–292.

Brown, J. M. and ElDabaje, R. (2008). PuMA: Bayesian analysis of partitioned (and unpartitioned) model adequacy. *Bioinformatics*, 25(4):537–538.

Brown, J. W. and Smith, S. A. (2017). The past sure is tense: on interpreting phylogenetic divergence time estimates. *bioRxiv*.

Chomicki, G., Ward, P. S., and Renner, S. S. (2015). Macroevolutionary assembly of ant/plant symbioses: *Pseudomyrmex* ants and their ant-housing plants in the Neotropics. *Proc. R. Soc. Lond. Ser. B. Biol. Sci.*, 282(1819):20152200.

Darling, D. C. and Sharkey, M. J. (1990). Taxonomic names, in insects from the Santana Formation, Lower Cretaceous, of Brazil. Chapter 7: Order Hymenoptera. *Bull. Amer. Mus. Nat. Hist.*,

195:123–153.

Dlussky, G. M. (1988). Ants of Sakhalin amber (Paleocene?). *Paleontolog. J.*, 22(1):50–61.

Dlussky, G. M. (1997). Genera of ants (Hymenoptera: Formicidae) from Baltic amber. *Paleontolog. J.*, 31:616–627.

Dlussky, G. M. (2009). The ant subfamilies Ponerinae, Cerapachyinae, and Pseudomyrmecinae (Hymenoptera, Formicidae) in the Late Eocene Ambers of Europe. *Paleontolog. J.*, 43(9):1043–1086.

Dlussky, G. M. and Perkovsky, E. E. (2002). Ants (Hymenoptera, Formicidae) from the Rovno Amber. [In Russian.]. *Vestn. Zool.*, 36(5):3–20.

Dlussky, G. M. and Radchenko, A. G. (2011). *Pristomyrmex rasnitsyni* sp. n., the first known fossil species of the ant genus *Pristomyrmex* mayr (Hymenoptera: Formicidae) from the Late Eocene Danish amber. *Russ. Entomol. J.*, 20(3):251–254.

Dlussky, G. M. and Rasnitsyn, A. P. (2003). Ants (Hymenoptera: Formicidae) of Formation Green River and some other Middle Eocene deposits of North America. *Russ. Entomol. J.*, 11(4):411–436.

Dlussky, G. M. and Rasnitsyn, A. P. (2009). Ants (Insecta: Vespida: Formicidae) in the Upper Eocene amber of central and eastern Europe. *Paleontolog. J.*, 43(9):1024–1042.

Dlussky, G. M., Rasnitsyn, A. P., and Perfilieva, K. S. (2015). The ants (Hymenoptera: Formicidae) of Bol'shaya Svetlovodnaya (Late Eocene of Sikhote-Alin, Russian Far East). *Cauc. Entomol. Bull.*, 11(1):131–152.

Dlussky, G. M., Wappler, T., and Wedmann, S. (2008). New middle Eocene formicid species from Germany and the evolution of weaver ants. *Acta Palaeontol. Polonica*, 53(4):615–626.

Doyle, V. P., Young, R. E., Naylor, G. J. P., and Brown, J. M. (2015). Can we identify genes with increased phylogenetic reliability? *Syst. Biol.*, 64(5):824–837.

Drummond, A. J. and Rambaut, A. (2007). BEAST: bayesian evolutionary analysis by sampling trees. *BMC Evol. Biol.*, 7(1):214.

Engel, M. S. (2008). The wasp family Rhopalosomatidae in mid-Cretaceous amber from Myanmar (Hymenoptera: Vespoidea). *J. Kansas Entomol. Soc.*, 81(3):168–174.

Engel, M. S., Ortega-Blanco, J., and Bennett, D. J. (2009). A remarkable tiphiiform wasp in mid-Cretaceous amber from Myanmar (Hymenoptera: Tiphiidae). *Trans. Kans. Acad. Sci.*, 112(1/2):1–6.

Faircloth, B. C., Branstetter, M. G., White, N. D., and Brady, S. G. (2014). Target enrichment of ultraconserved elements from arthropods provides a genomic perspective on relationships among Hymenoptera. *Mol. Ecol. Resour.*, 15(3):489–501.

Foster, P. (2004). Modeling compositional heterogeneity. *Syst. Biol.*, 53(3):485–495.

Frandsen, P. B., Calcott, B., Mayer, C., and Lanfear, R. (2015). Automatic selection of partitioning schemes for phylogenetic analyses using iterative k-means clustering of site rates. *BMC Evol. Biol.*, 15(1):13.

636 Gascuel, O. (1997). BIONJ: an improved version of the NJ algorithm based on a simple model of
637 sequence data. *Mol. Biol. Evol.*, 14(7):685–695.

638 Goremykin, V. V., Nikiforova, S. V., Cavalieri, D., Pindo, M., and Lockhart, P. (2015). The root of
639 flowering plants and total evidence. *Syst. Biol.*, 64(5):879–891.

640 Grimaldi, D. and Agosti, D. (2000). A formicine in New Jersey Cretaceous amber (Hymenoptera:
641 Formicidae) and early evolution of the ants. *Proc. Natl. Acad. Sci. U.S.A.*, 97:13678–13683.

642 Guindon, S., Dufayard, J. F., Lefort, V., Anisimova, M., Hordijk, W., and Gascuel, O. (2010).
643 New algorithms and methods to estimate maximum-likelihood phylogenies: Assessing the per-
644 formance of PhyML 3.0. *Syst. Biol.*, 59(3):307–321.

645 Heath, T. A., Huelsenbeck, J. P., and Stadler, T. (2014). The fossilized birth-death process for
646 coherent calibration of divergence-time estimates. *Proc. Natl. Acad. Sci. U.S.A.*, 111(29):E2957–
647 E2966.

648 Höhna, S., Stadler, T., Ronquist, F., and Britton, T. (2011). Inferring speciation and extinction rates
649 under different sampling schemes. *Mol. Biol. Evol.*, 28(9):2577–2589.

650 Hölldobler, B. and Wilson, E. O. (1990). *The ants*. Harvard University Press.

651 Huelsenbeck, J. P. and Hillis, D. M. (1993). Success of phylogenetic methods in the four-taxon
652 case. *Syst. Biol.*, 42(3):247–264.

653 Jayaswal, V., Wong, T. K. F., Robinson, J., Poladian, L., and Jermiin, L. S. (2014). Mixture models
654 of nucleotide sequence evolution that account for heterogeneity in the substitution process across
655 sites and across lineages. *Syst. Biol.*, 63(5):726–742.

656 Jermiin, L., Ho, S. Y., Ababneh, F., Robinson, J., and Larkum, A. W. (2004). The biasing effect
657 of compositional heterogeneity on phylogenetic estimates may be underestimated. *Syst. Biol.*,
658 53(4):638–643.

659 Kugler, J. (1987). The Leptanillinae (Hymenoptera: Formicidae) of Israel and a description of a
660 new species from India. *Isr. J. Entomol.*, 20:45–57.

661 Kück, P., Hita Garcia, F., Misof, B., and Meusemann, K. (2011). Improved phylogenetic anal-
662 yses corroborate a plausible position of *Martialis heureka* in the ant tree of life. *PLoS ONE*
663 *(doi:10.1371/journal.pone.0021031)*, 6:e21031.

664 Lanfear, R., Frandsen, P. B., Wright, A. M., Senfeld, T., and Calcott, B. (2017). PartitionFinder
665 2: new methods for selecting partitioned models of evolution for molecular and morphological
666 phylogenetic analyses. *Mol. Biol. Evol.*, 34(3):772–773.

667 Lapolla, J. S. and Greenwalt, D. E. (2015). Fossil ants (Hymenoptera: Formicidae) of the Middle
668 Eocene Kishenehn Formation. *Sociobiology*, 62(2):163–174.

669 Lelej, A. S. (1986). Males of the genus *Protomutilla* (Hymenoptera, Mutillidae) from Baltic amber.
670 *Paleontol. Zh.*, 4:104–106.

671 Lucky, A., Trautwein, M. D., Guénard, B. S., Weiser, M. D., and Dunn, R. R. (2013). Tracing the
672 rise of ants - out of the ground. *PLoS ONE*, 8(12):e84012.

673 MacKay, W. P. (1991). *Anochetus brevidentatus*, new species, a second fossil Odontomachiti ant

(Hymenoptera: Formicidae). *J. N. Y. Entomol. Soc.*, 99(1):138–140.

Maddison, D. R. and Maddison, W. P. (2005). MacClade 4., v. 4.08 for OSX.

Mayr, G. (1868). Die Ameisen des baltischen Bernsteins. *Beitr. Naturkd. Preuss.*, 1:1–102.

McKellar, R. C., Glasier, J. R. N., and Engel, M. S. (2013). New ants (Hymenoptera: Formicidae: Dolichoderinae) from Canadian Late Cretaceous amber. *Bull. Geosci.*, 88(3):583–594.

Minh, B. Q., Nguyen, M. A. T., and von Haeseler, A. (2013). Ultrafast approximation for phylogenetic bootstrap. *Mol. Biol. Evol.*, 30(5):1188–1195.

Moreau, C. S. and Bell, C. D. (2013). Testing the museum versus cradle tropical biological diversity hypothesis: phylogeny, diversification, and ancestral biogeographic range evolution of the ants. *Evolution*, 67(8):2240–2257.

Moreau, C. S., Bell, C. D., Vila, R., Archibald, S. B., and Pierce, N. E. (2006). Phylogeny of the ants: diversification in the age of angiosperms. *Science*, 312:101–104.

Nguyen, L.-T., Schmidt, H. A., von Haeseler, A., and Minh, B. Q. (2014). IQ-TREE: a fast and effective stochastic algorithm for estimating maximum-likelihood phylogenies. *Mol. Biol. Evol.*, 32(1):268–274.

Nguyen, N. D., Mirarab, S., Kumar, K., and Warnow, T. (2015). Ultra-large alignments using phylogeny-aware profiles. *Genome Biol.*, 16(1):124.

Ogata, K., Terayama, M., and Masuko, K. (1995). The ant genus *Leptanilla:* discovery of the worker-associated male of *L. japonica,* and a description of a new species from Taiwan (Hymenoptera: Formicidae: Leptanillinae). *Syst. Entomol.*, 20:27–34.

Ohl, M. (2004). The first fossil representative of the wasp genus *Dolichurus*, with a review of fossil Ampulicidae (Hymenoptera: Apoidea). *J. Kansas Entomol. Soc.*, 77(4):332–342.

Perrichot, V. (2015). A new species of *Baikuris* (Hymenoptera: Formicidae: Sphecomyrminae) in mid-Cretaceous amber from France. *Cretaceous Res.*, 52(B):585–590.

Perrichot, V., Lacau, S., Néraudeau, D., and Nel, A. (2008). Fossil evidence for the early ant evolution. *Naturwissenschaften*, 95(2):85–90.

Peters, R. S., Krogmann, L., Mayer, C., Donath, A., Gunkel, S., Meusemann, K., Kozlov, A., Podsiadlowski, L., Petersen, M., Lanfear, R., Diez, P. A., Heraty, J., Kjer, K. M., Klopfstein, S., Meier, R., Polidori, C., Schmitt, T., Liu, S., Zhou, X., Wappler, T., Rust, J., Misof, B., and Niehuis, O. (2017). Evolutionary history of the hymenoptera. *Curr. Biol.*, 27(7):1013–1018.

Philippe, H. and Roure, B. (2011). Difficult phylogenetic questions: more data, maybe; better methods, certainly. *BMC Biol.*, 9(1):91.

Pie, M. R. and Feitosa, R. M. (2015). Relictual ant lineages (Hymenoptera: Formicidae) and their evolutionary implications. *Myrmecol. News*, 22:55–58.

Pilgrim, E. M., Dohlen, C. D. V., and Pitts, J. P. (2008). Molecular phylogenetics of Vespoidea indicate paraphyly of the superfamily and novel relationships of its component families and subfamilies. *Zool. Scripta*, 37(5):539–560.

Poinar, G. O. (2009). *Melittosphex* (Hymenoptera: Melittosphecidae), a primitive bee and not a wasp. *Palaeontology*, 52(2):483–484.

Poinar, G. O. and Danforth, B. N. (2006). A fossil bee from Early Cretaceous Burmese amber. *Science*, 314(5799):614.

Rabeling, C., Brown, J. M., and Verhaagh, M. (2008). Newly discovered sister lineage sheds light on early ant evolution. *Proc. Natl. Acad. Sci. U.S.A.*, 105:14913–14917.

Radchenko, A. G., Elmes, G. W., and Dlussky, G. (2007). The ants of the genus *Myrmica* (Hymenoptera, Formicidae) from Baltic and Saxonian amber (Late Eocene). *J. Paleontol.*, 81(6):1494–1501.

Rasnitsyn, A. P. and Jarzembowski, E. A. (1998). Systematic part, in wasps (Insecta: Vespida = Hymenoptera) from the Purbeck and Wealden Supergroups (Lower Cretaceous) of southern England and their biostratigraphical and palaeoenvironmental significance. *Cretaceous Res.*, 19(3/4):329–391.

Rasnitsyn, A. P. and Martínez-Delclòs, X. (2000). Wasps (Insecta: Vespida = Hymenoptera) from the Early Cretaceous of Spain. *Acta Geol. Hisp.*, 35(1-2):65–96.

Rodriguez, J., Waichert, C., Dohlen, C. D. V., Jr, G. P., and Pitts, J. P. (2016). Eocene and not Cretaceous origin of spider wasps: fossil evidence from amber. *Acta Palaeontol. Polonica*, 61(1):89–96.

Ronquist, F., Teslenko, M., van der Mark, P., Ayres, D. L., Darling, A., Höhna, S., Larget, B., Liu, L., Suchard, M. A., and Huelsenbeck, J. P. (2012). MrBayes 3.2: efficient bayesian phylogenetic inference and model choice across a large model space. *Syst. Biol.*, 61(3):539–542.

Rust, J. and Andersen, N. M. (1999). Giant ants from the Paleogene of Denmark with a discussion of the fossil history and early evolution of ants (Hymenoptera: Formicidae). *Zool. J. Linn. Soc.*, 125(3):331–348.

Sanderson, M. J. (2002). Estimating absolute rates of molecular evolution and divergence times: a penalized likelihood approach. *Mol. Biol. Evol.*, 19(1):101–109.

Schmidt, C. (2013). Molecular phylogenetics of ponerine ants (Hymenoptera: Formicidae: Ponerinae). *Zootaxa*, 3647:201–250.

Schmidt, C. A. and Shattuck, S. O. (2014). The higher classification of the ant subfamily Ponerinae (Hymenoptera: Formicidae), with a review of ponerine ecology and behavior. *Zootaxa*, 3817:1–242.

Stamatakis, A. (2014). RAxML version 8: a tool for phylogenet. anal. and post-analysis of large phylogenies. *Bioinformatics*, 30(9):1312–1313.

Takezaki, N. and Nishihara, H. (2016). Resolving the phylogenetic position of coelacanth: the closest relative is not always the most appropriate outgroup. *Genome Biol. Evol.*, 8(4):1208–1221.

Thompson, J. D., Gibson, T. J., Plewniak, F., Jeanmougin, F., and Higgins, D. G. (1997). The CLUSTAL_x windows interface: flexible strategies for multiple sequence alignment aided by quality analysis tools. *Nucleic Acids Res.*, 25(24):4876–4882.

Urbani, C. B. (1980). *Anochetus corayi* n. sp., the first fossil Odontomachiti ant. (Amber Collection Stuttgart: Hymenoptera, Formicidae. II: Odontomachiti). *Stuttg. Beitr. Naturkd. Ser. B (Geol. Paläontol.)*, (55):1–6.

Urbani, C. B. and Andrade, M. L. D. (2003). The ant genus *Proceratium* in the extant and fossil rec. (Hymenoptera: Formicidae). *Mus. Reg. Sci. Nat. Monogr. (Turin)*, 36:1–492.

Wappler, T., Dlussky, G. M., Engel, M. S., Prokop, J., and Knor, S. (2014). A new trap-jaw ant species of the genus *Odontomachus* (Hymenoptera: Formicidae: Ponerinae) from the Early Miocene (Burdigalian) of the Czech Republic. *Paläntolog. Z.*, 88(4):495–502.

Ward, P. S. (2014). The phylogeny and evolution of ants. *Annu. Rev. Ecol. Evol. Syst.*, 45:23–43.

Ward, P. S., Brady, S. G., Fisher, B. L., and Schultz, T. R. (2010). Phylogeny and biogeography of dolichoderine ants: effects of data partitioning and relict taxa on historical inference. *Syst. Biol.*, 59:342–362.

Ward, P. S., Brady, S. G., Fisher, B. L., and Schultz, T. R. (2015). The evolution of myrmicine ants: phylogeny and biogeography of a hyperdiverse ant clade (Hymenoptera: Formicidae). *Syst. Entomol.*, 40(1):61–81.

Ward, P. S. and Fisher, B. L. (2016). Tales of dracula ants: the evolutionary history of the ant subfamily Amblyoponinae (Hymenoptera: Formicidae). *Syst. Entomol.*, 41(3):683–693.

Wheeler, G. C. and Wheeler, E. W. (1930). Two new ants from Java. *Psyche (Cambridge)*, 37:193–201.

Wheeler, W. M. (1915). The ants of the Baltic amber. *Schr. Phys.-Ökon. Ges. Königsb.*, (55):1–142.

Wilson, E. O. (2004). The biogeography of the West Indian ants (Hymenoptera: Formicidae). In Liebherr, J. K., editor, *Zoogeography of Caribbean insects*, chapter 10, pages 266–290. Cornell University Press, Ithaca, New York.

Zhang, C., Stadler, T., Klopfstein, S., Heath, T. A., and Ronquist, F. (2016). Total-evidence dating under the fossilized birth–death process. *Syst. Biol.*, 65(2):228–249.

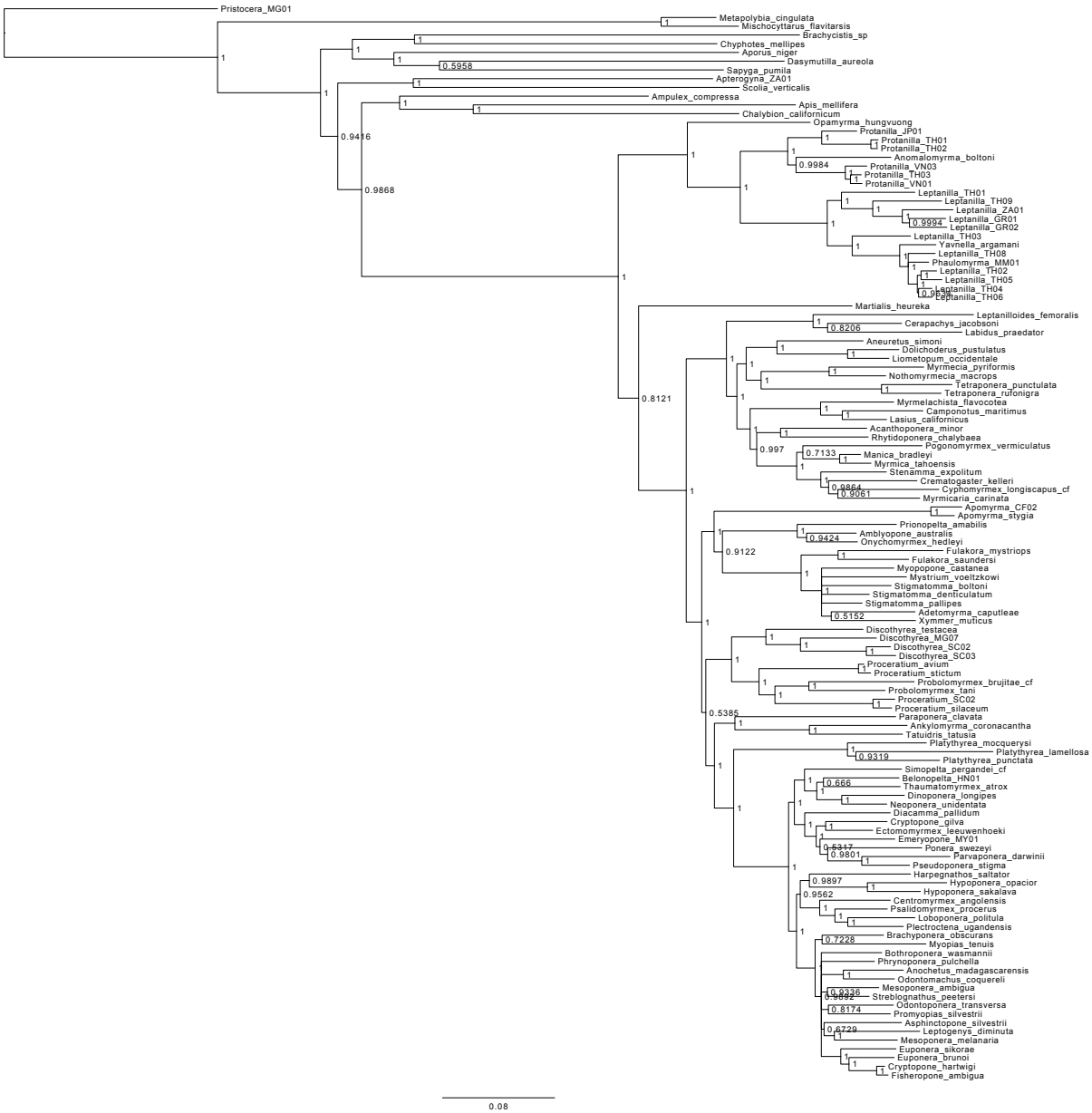

Supplementary Figure 1: Bayesian consensus tree inferred under greedy partitioning strategy for full data set.

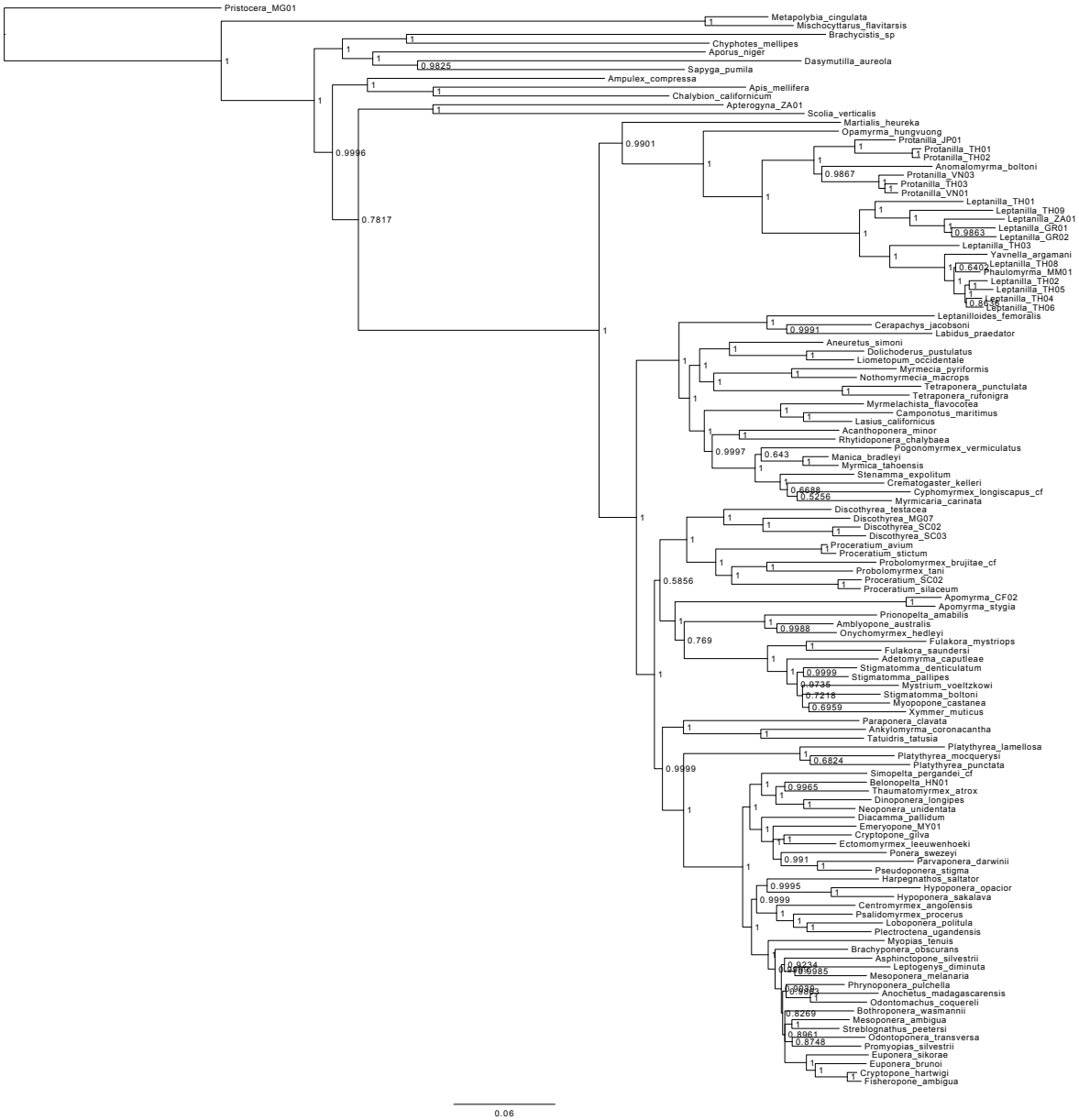

Supplementary Figure 2: Bayesian consensus tree inferred under k-means partitioning strategy for full data set.

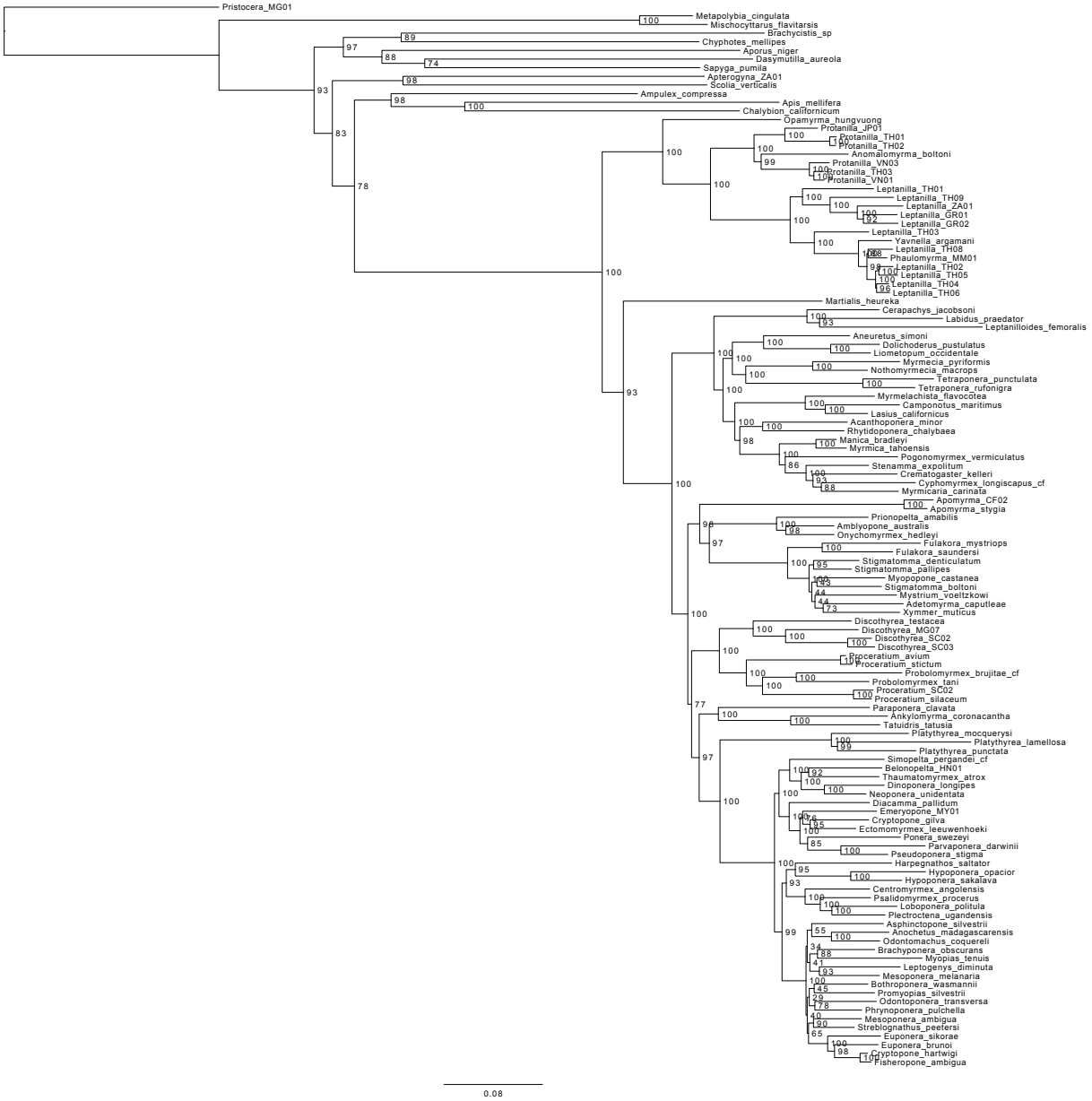

Supplementary Figure 3: Maximum-likelihood tree inferred under greedy partitioning strategy for full data set.

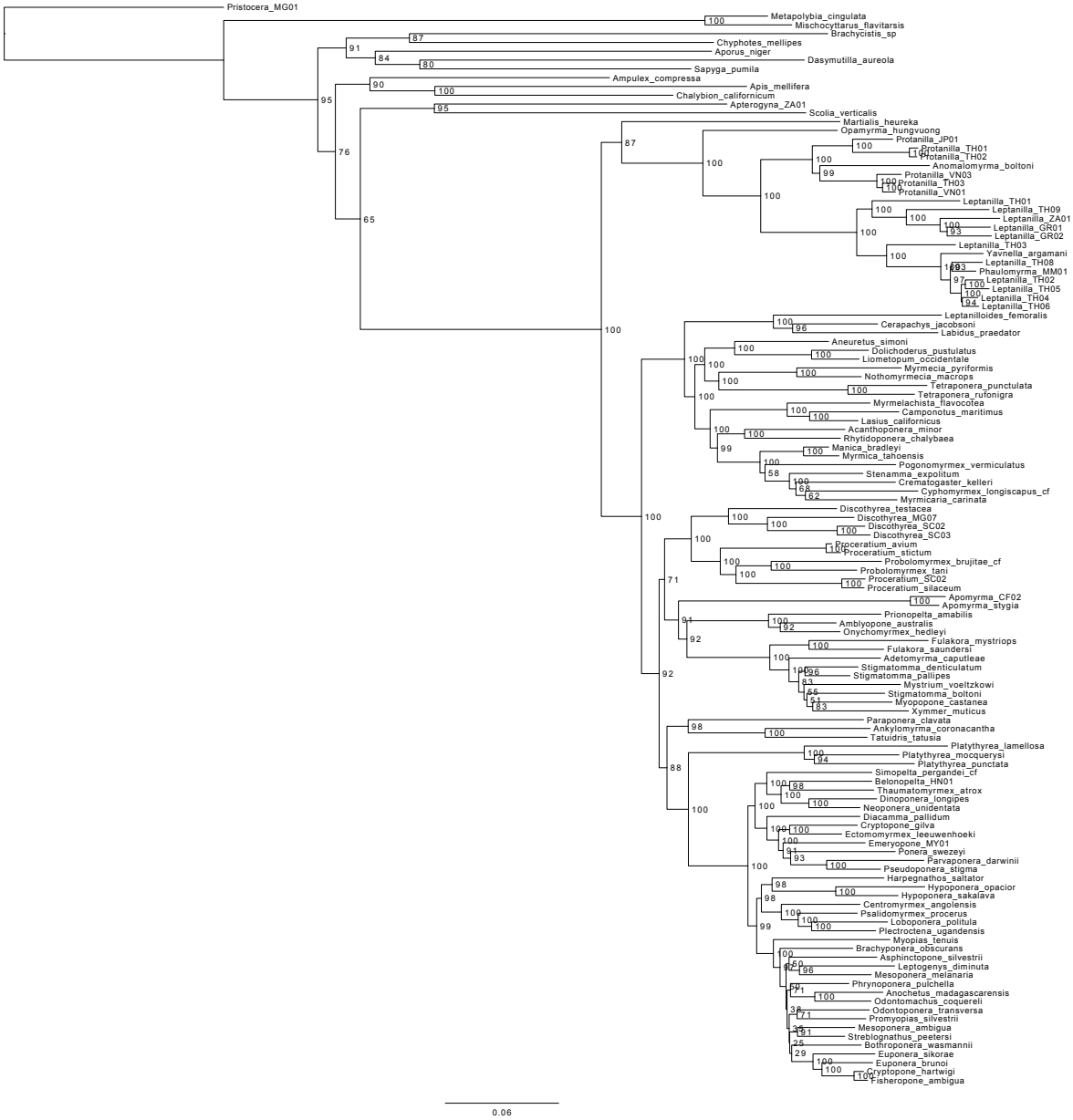

Supplementary Figure 4: Maximum-likelihood tree inferred under k-means partitioning strategy for full data set.

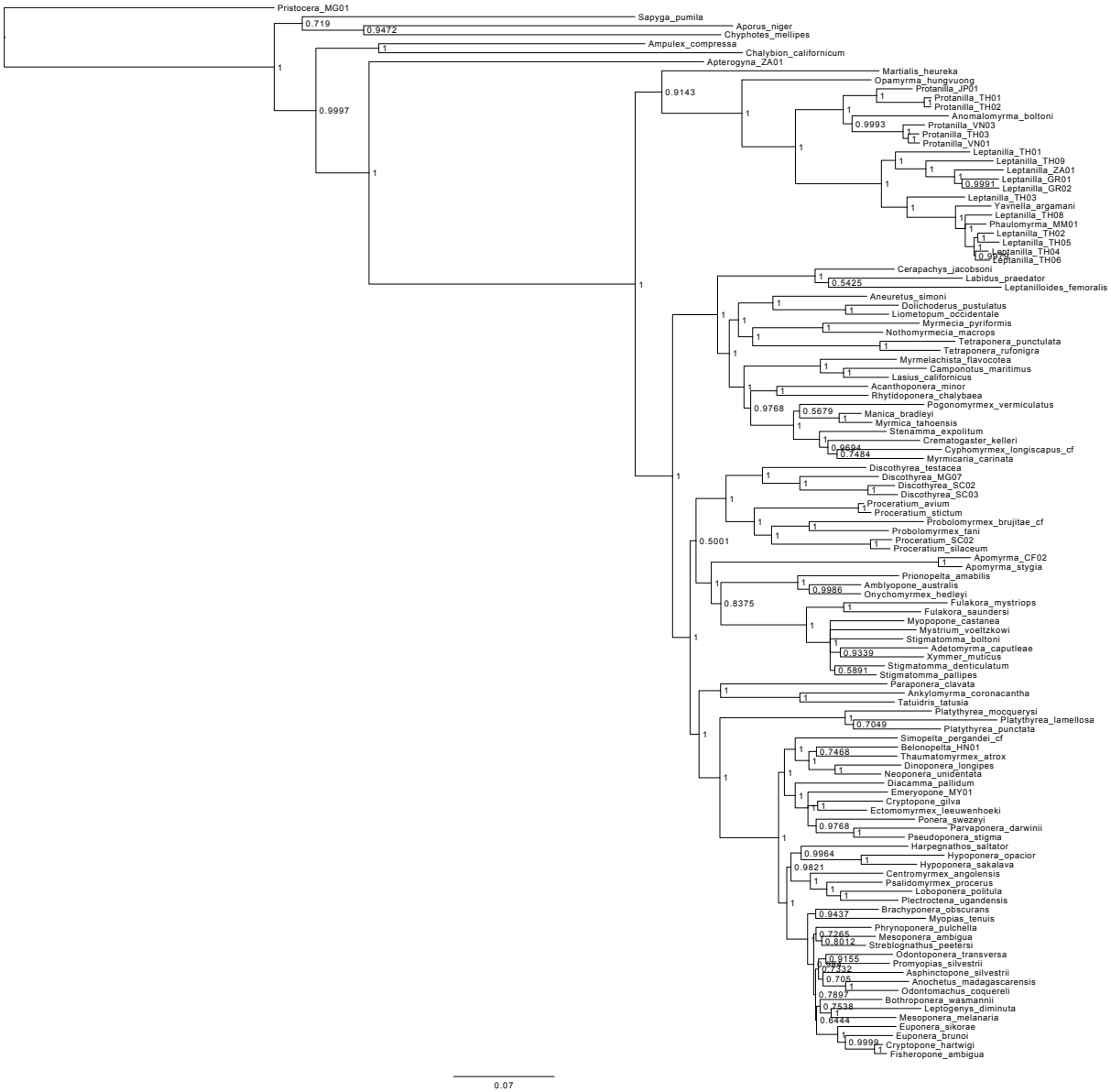

Supplementary Figure 5: Bayesian consensus tree inferred under greedy partitioning strategy for datset with AT-rich outgroups removed.

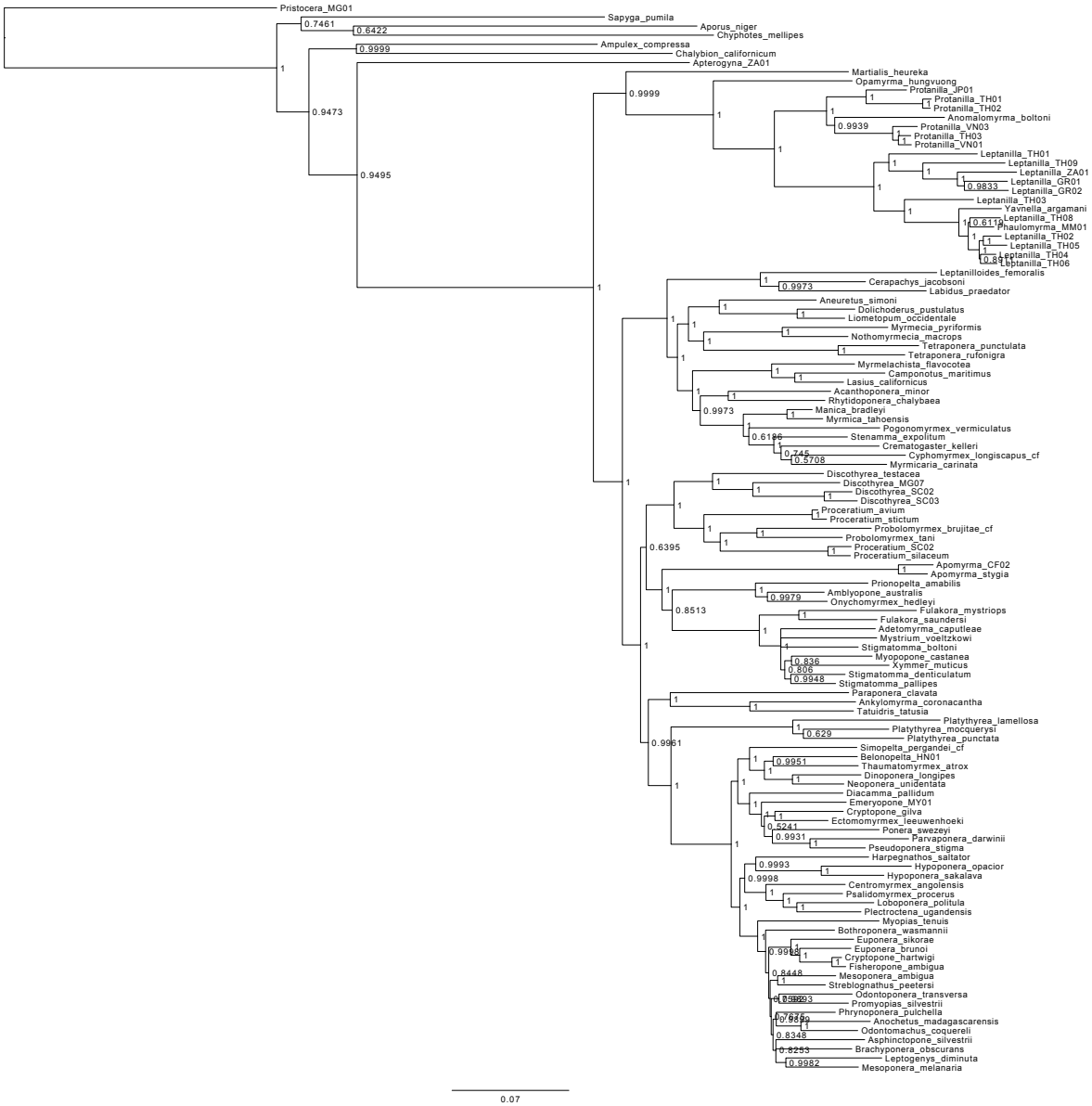

Supplementary Figure 6: Bayesian consensus tree inferred under k-means partitioning strategy for datset with AT-rich outgroups removed.

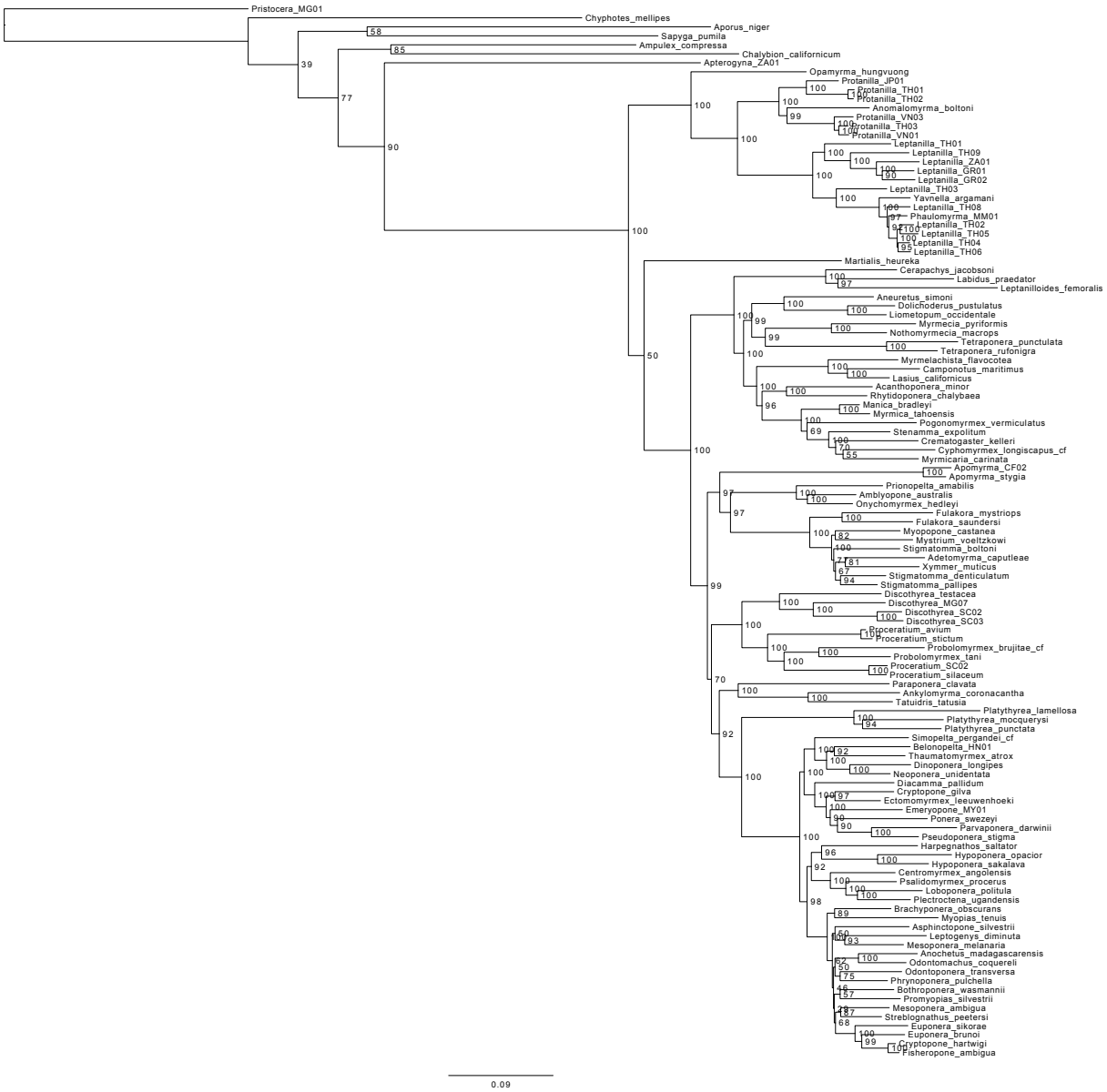

Supplementary Figure 7: Maximum-likelihood tree inferred under greedy partitioning strategy for datset with AT-rich outgroups removed.

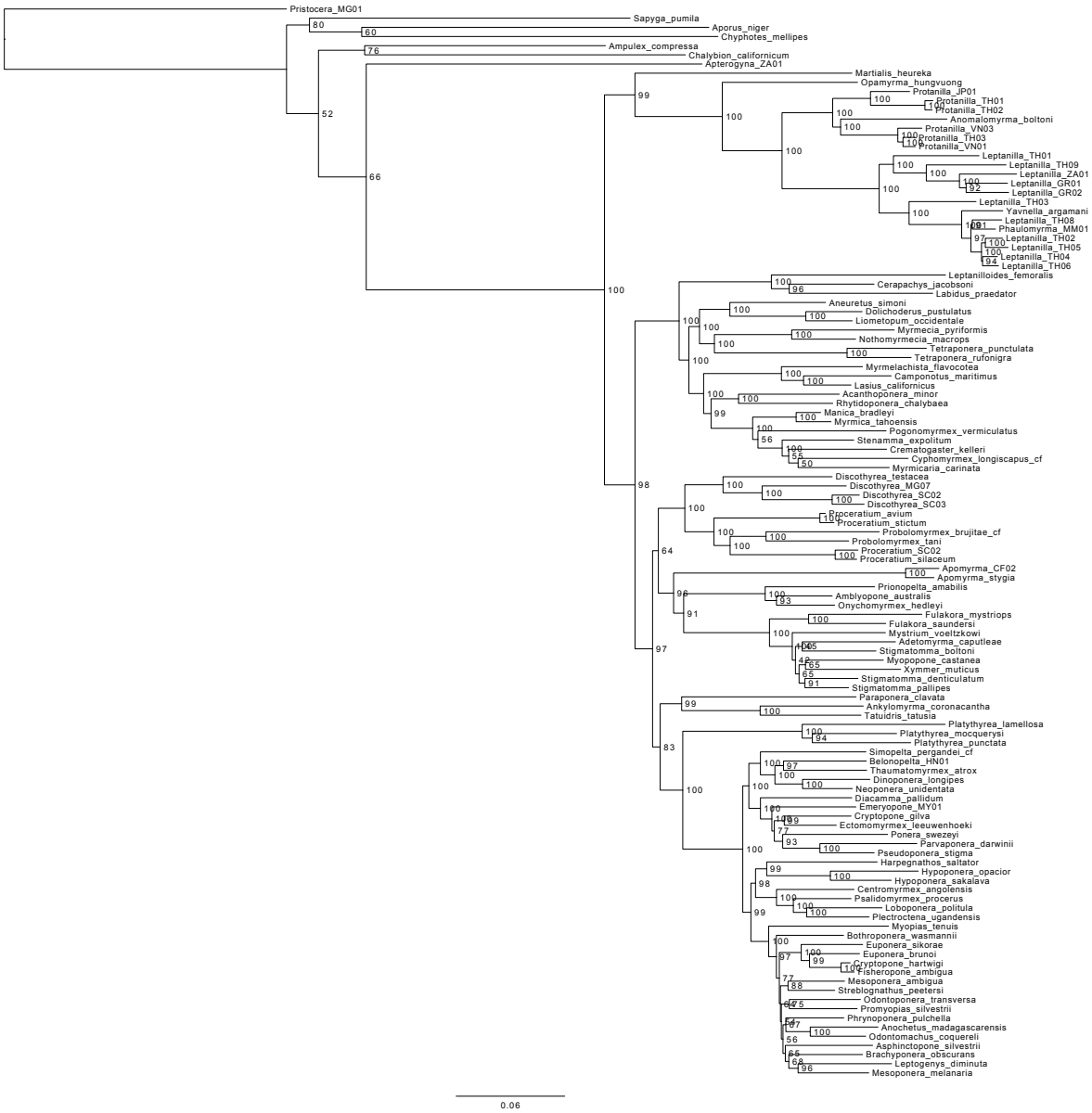

Supplementary Figure 8: Maximum-likelihood tree inferred under k-means partitioning strategy for datset with AT-rich outgroups removed.

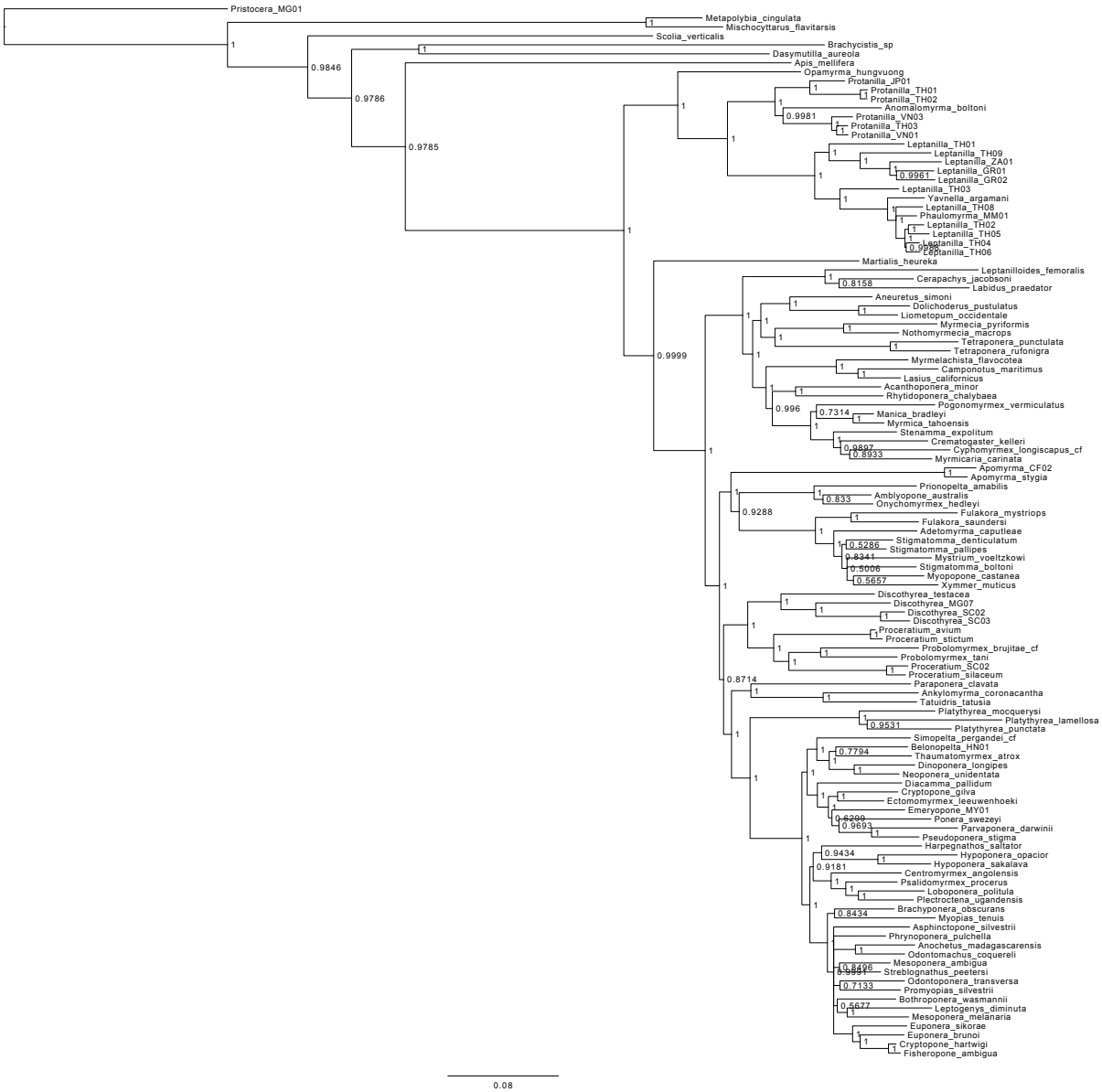

Supplementary Figure 9: Bayesian consensus tree inferred under greedy partitioning strategy for datset with GC-rich outgroups removed.

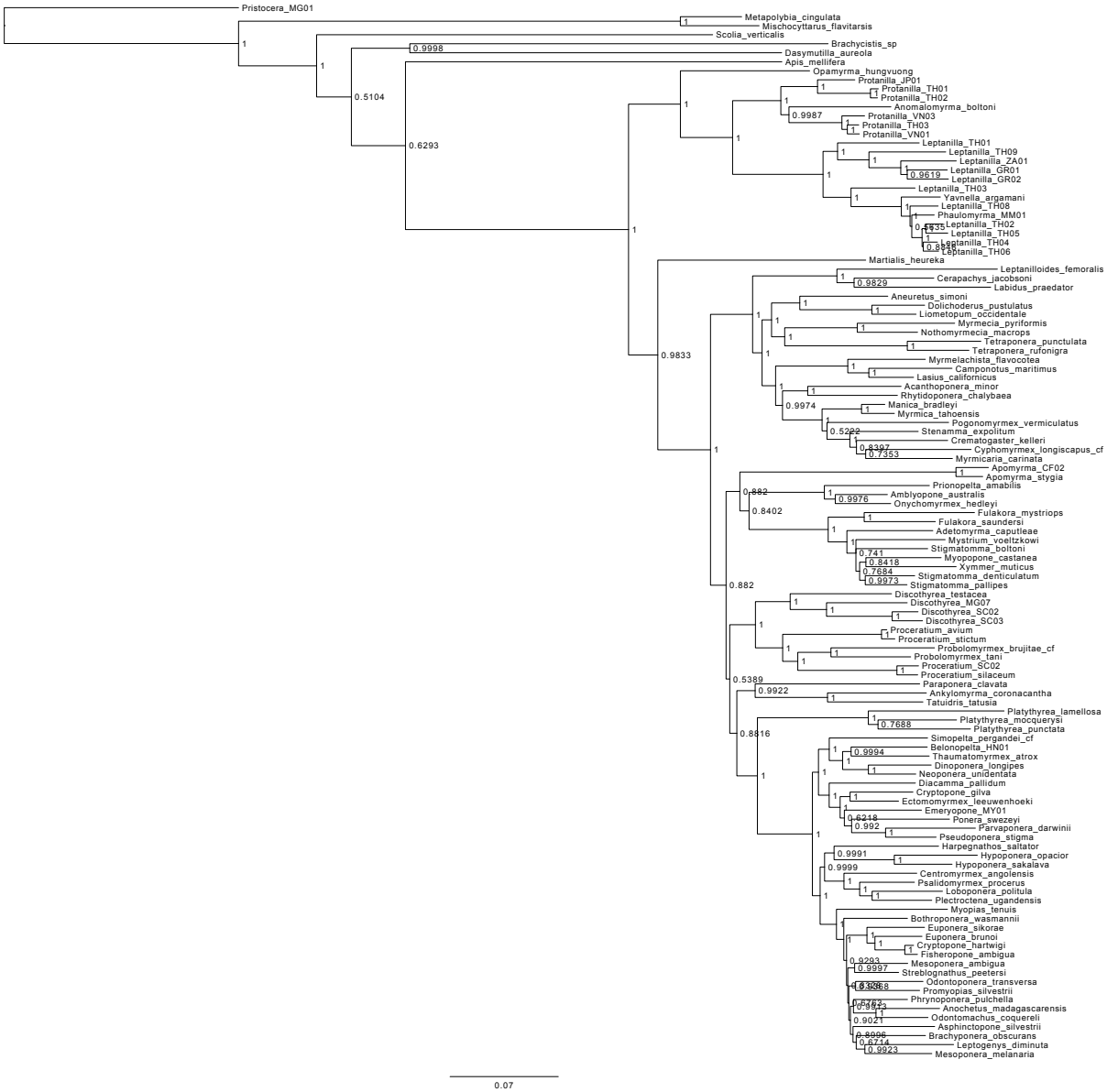

Supplementary Figure 10: Bayesian consensus tree inferred under k-means partitioning strategy for datset with GC-rich outgroups removed.

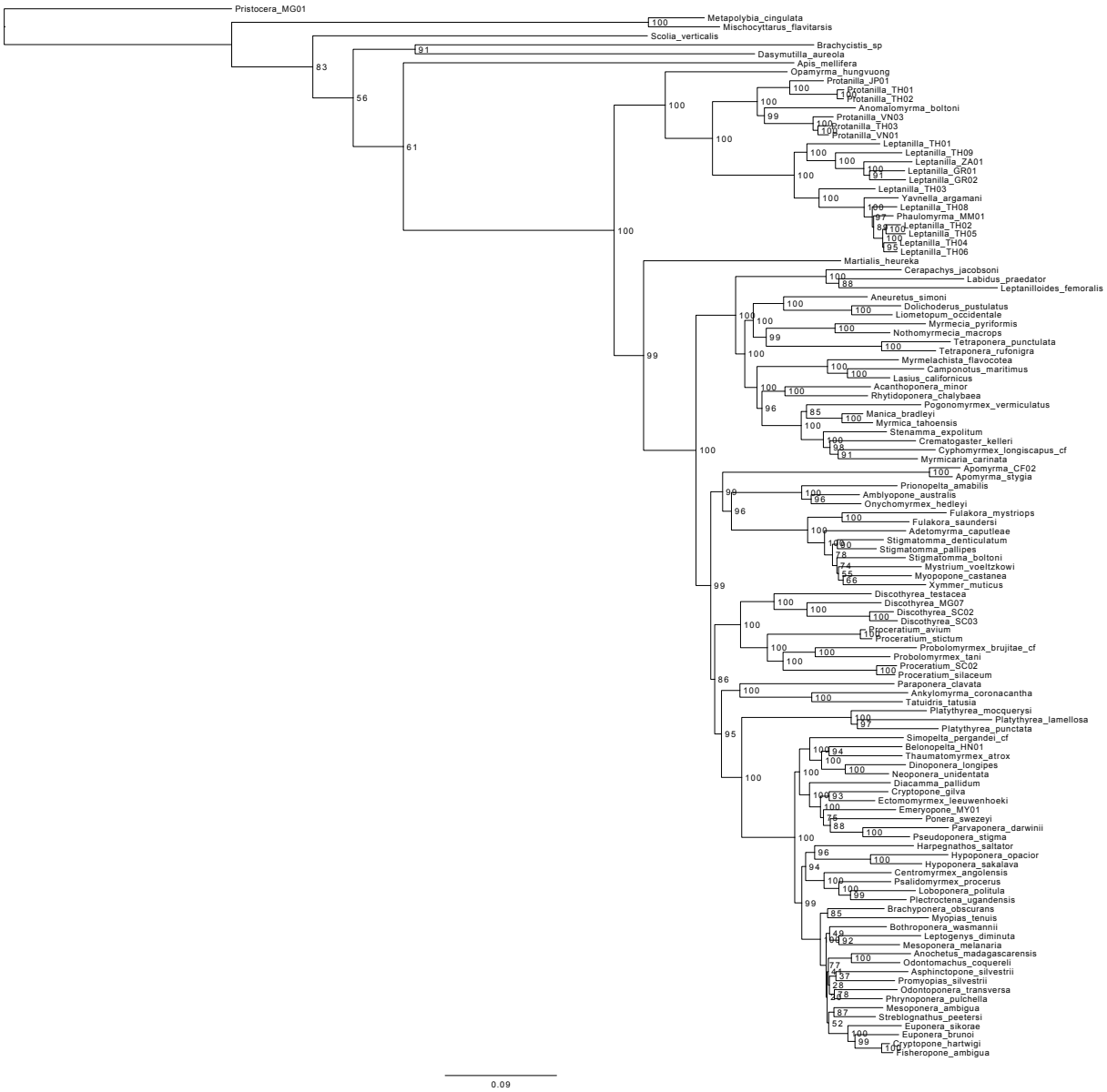

Supplementary Figure 11: Maximum-likelihood tree inferred under greedy partitioning strategy for datset with GC-rich outgroups removed.

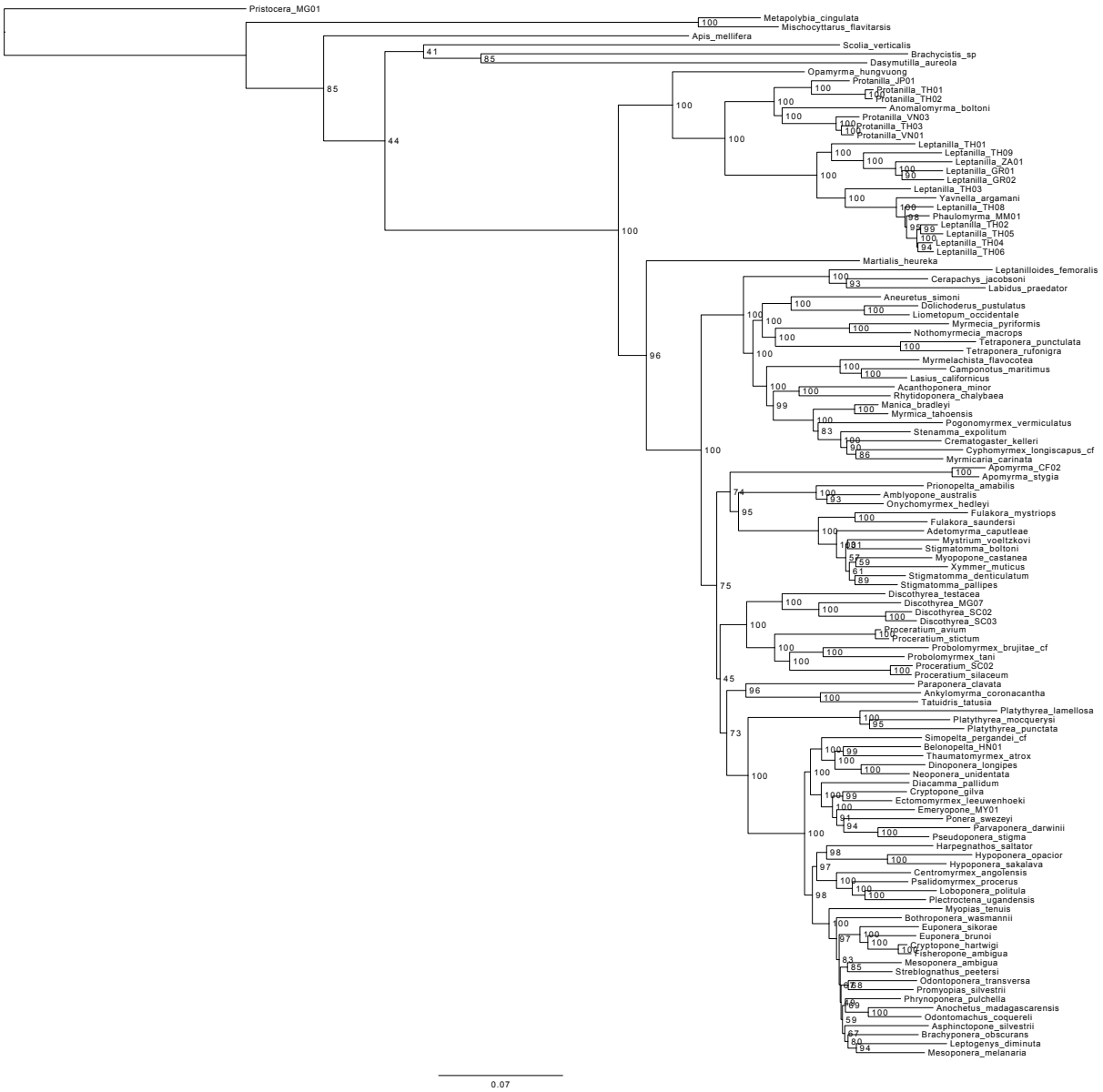

Supplementary Figure 12: Maximum-likelihood tree inferred under k-means partitioning strategy for datset with GC-rich outgroups removed.

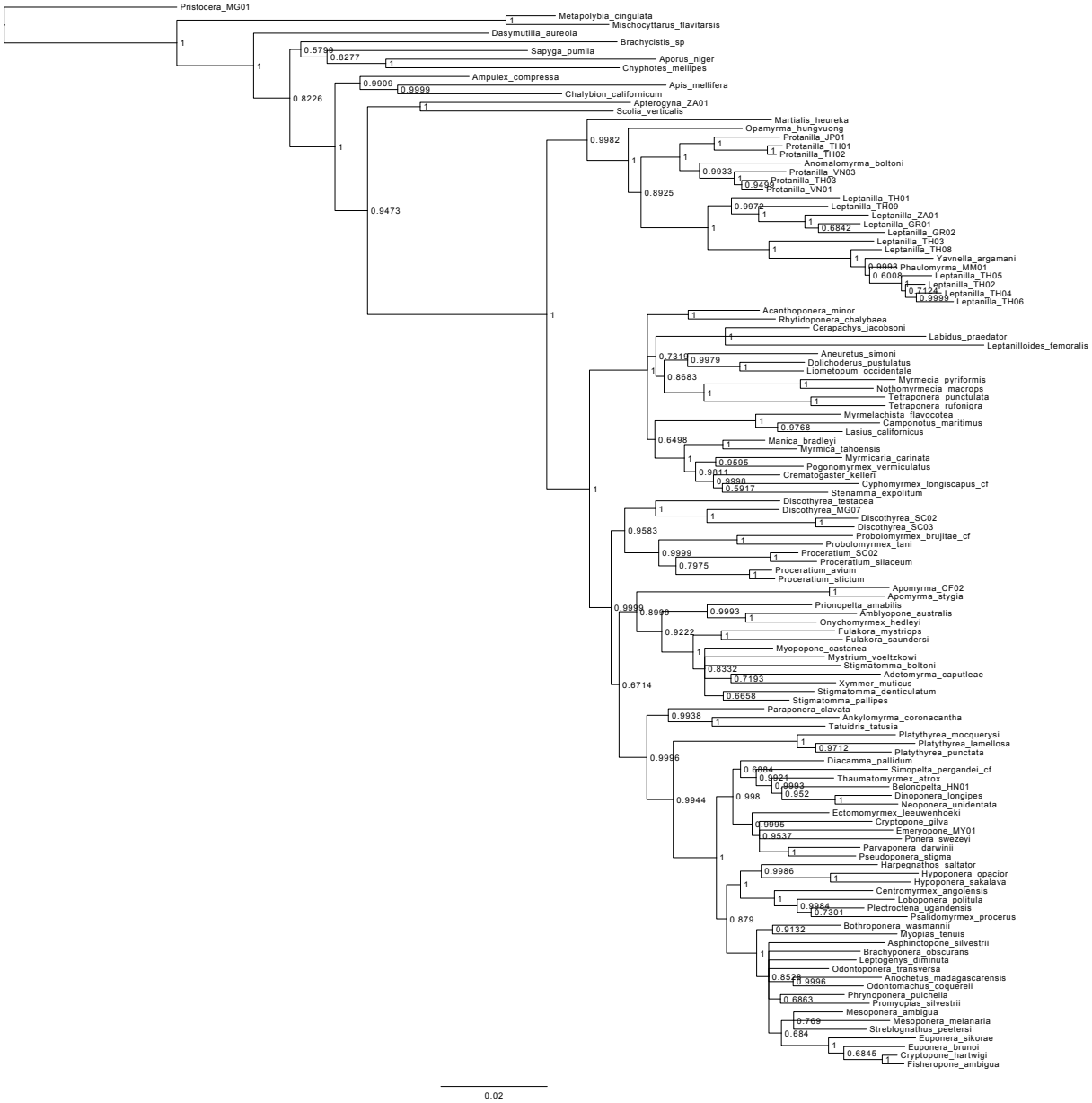

Supplementary Figure 13: Bayesian consensus tree inferred under greedy partitioning strategy for compositionally homogeneous datset.

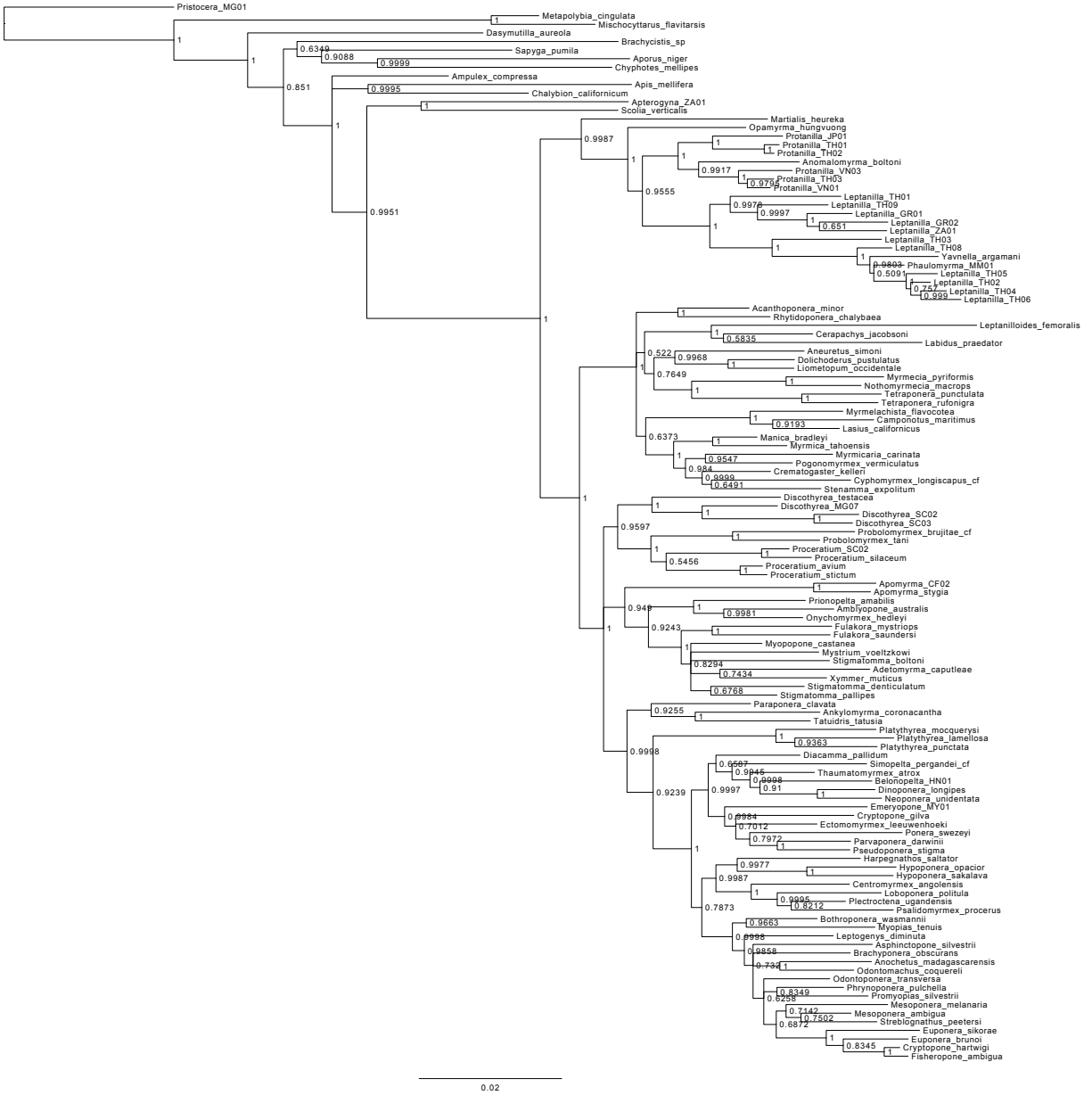

Supplementary Figure 14: Bayesian consensus tree inferred under k-means partitioning strategy for compositionally homogeneous datset.

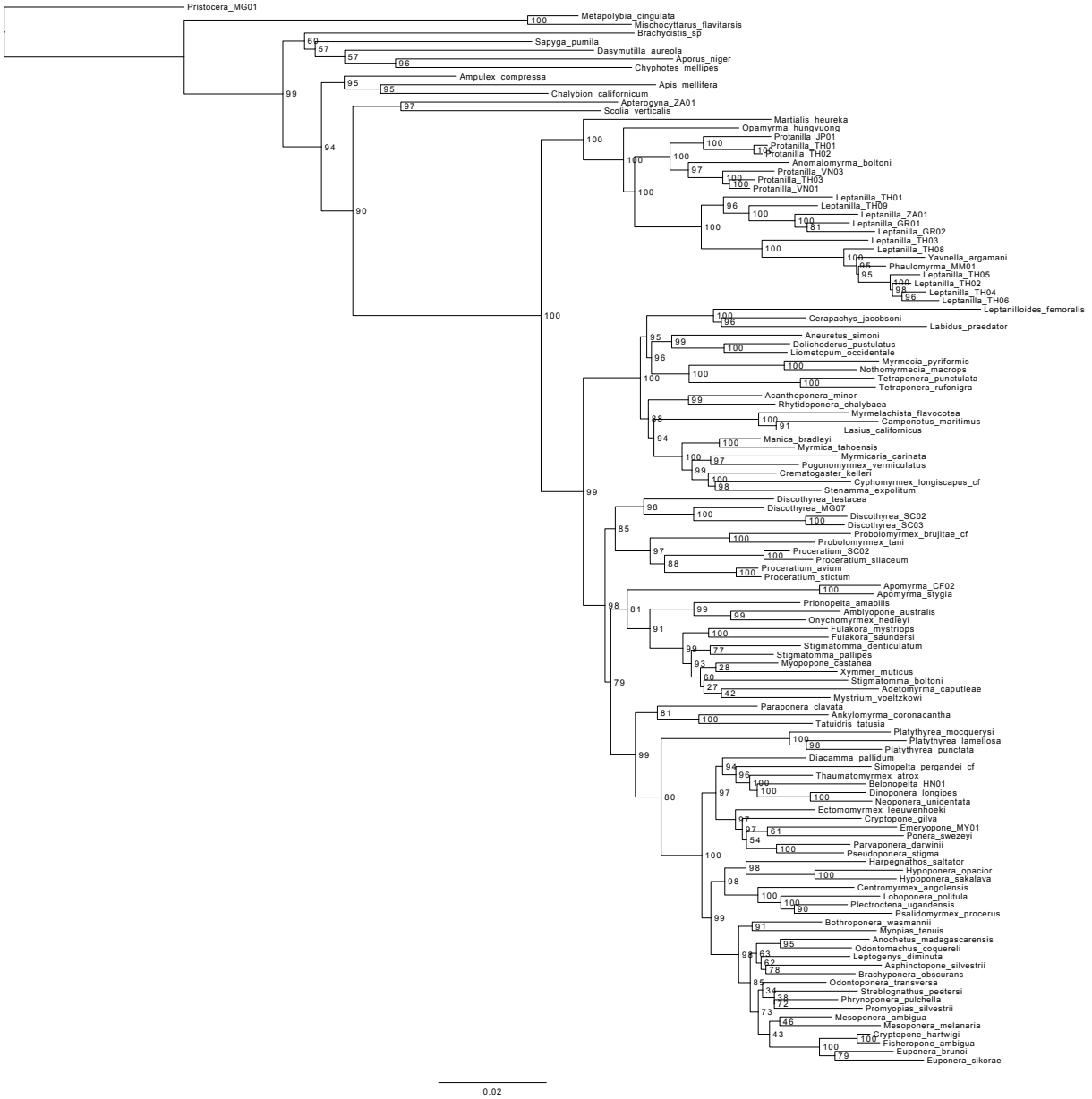

Supplementary Figure 15: Maximum-likelihood tree inferred under greedy partitioning strategy for compositionally homogeneous datset.

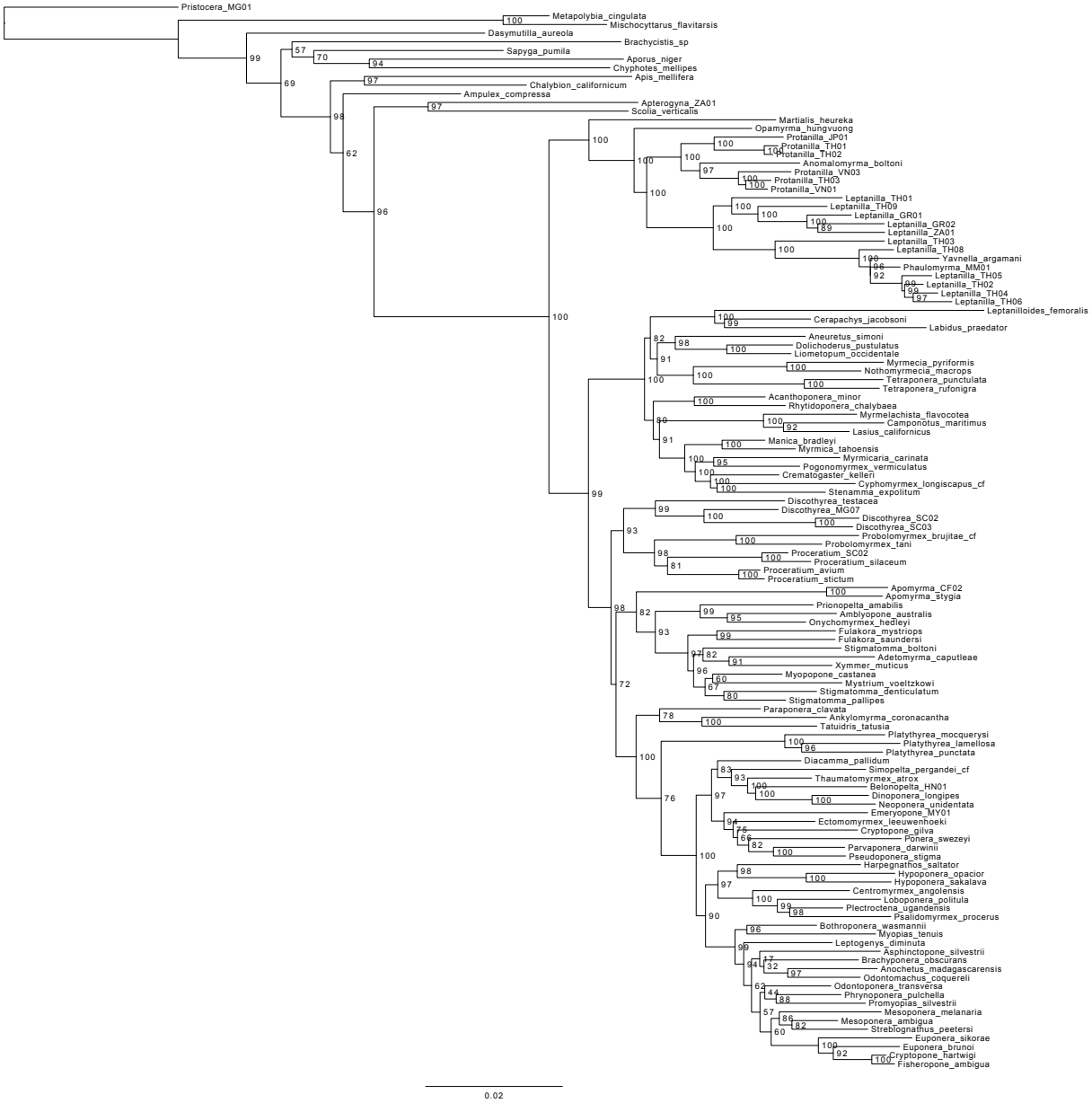

Supplementary Figure 16: Maximum-likelihood tree inferred under k-means partitioning strategy for compositionally homogeneous datset.

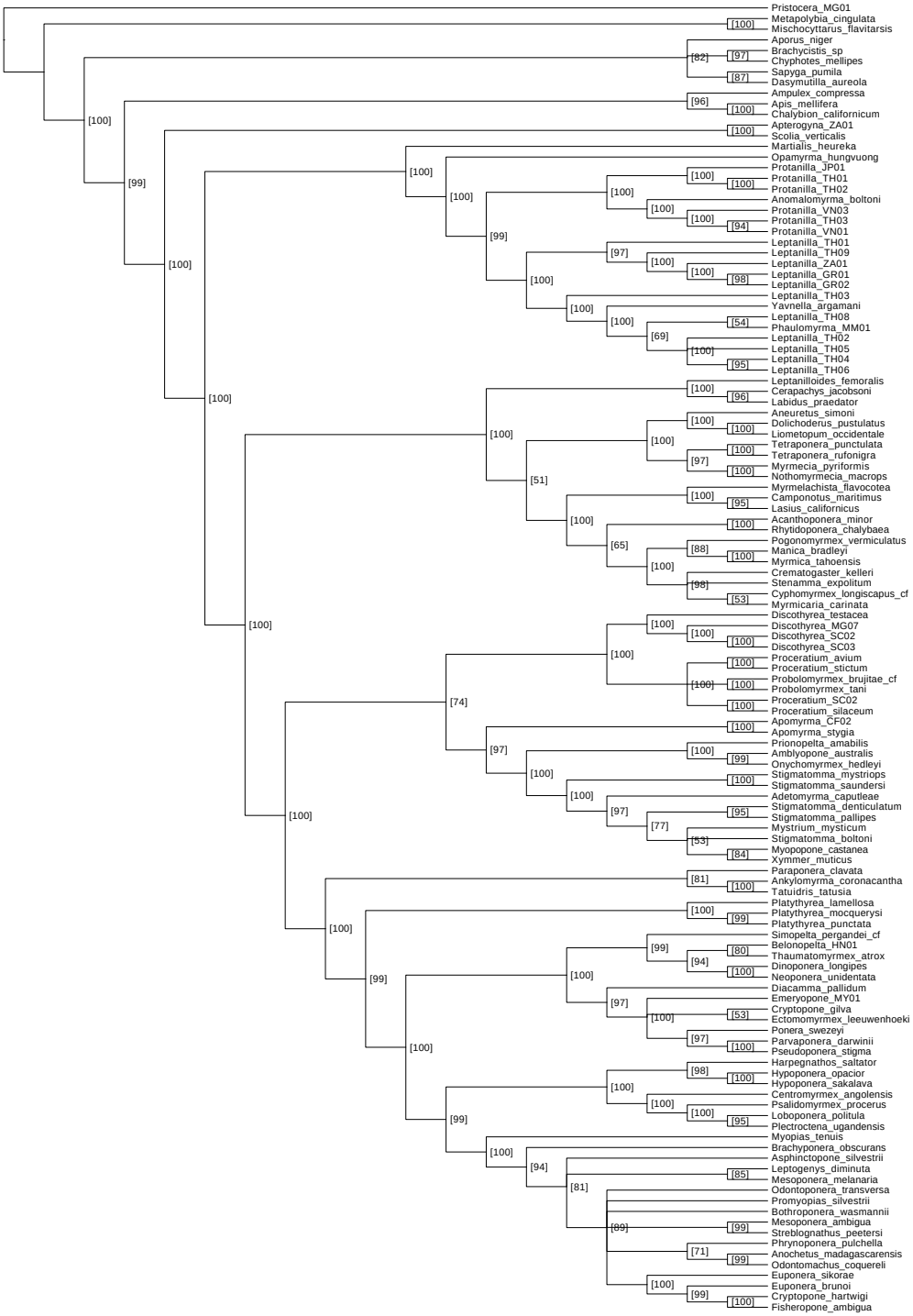

Supplementary Figure 17: Majority-rule consensus of maximum-likelihood trees inferred from 100 simulated alignments imitating first codon positions.

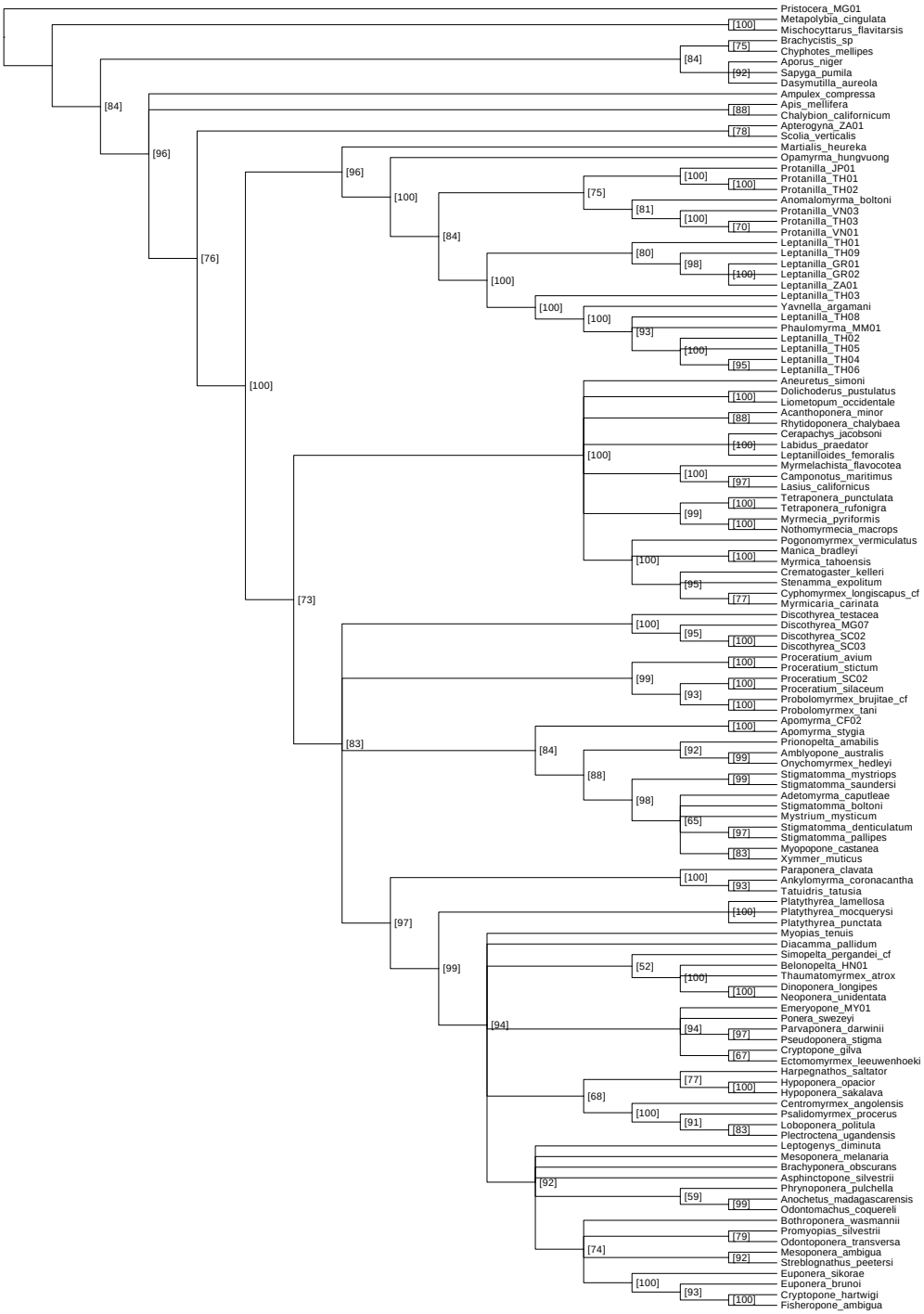

Supplementary Figure 18: Majority-rule consensus of maximum-likelihood trees inferred from 100 simulated alignments imitating second codon positions.

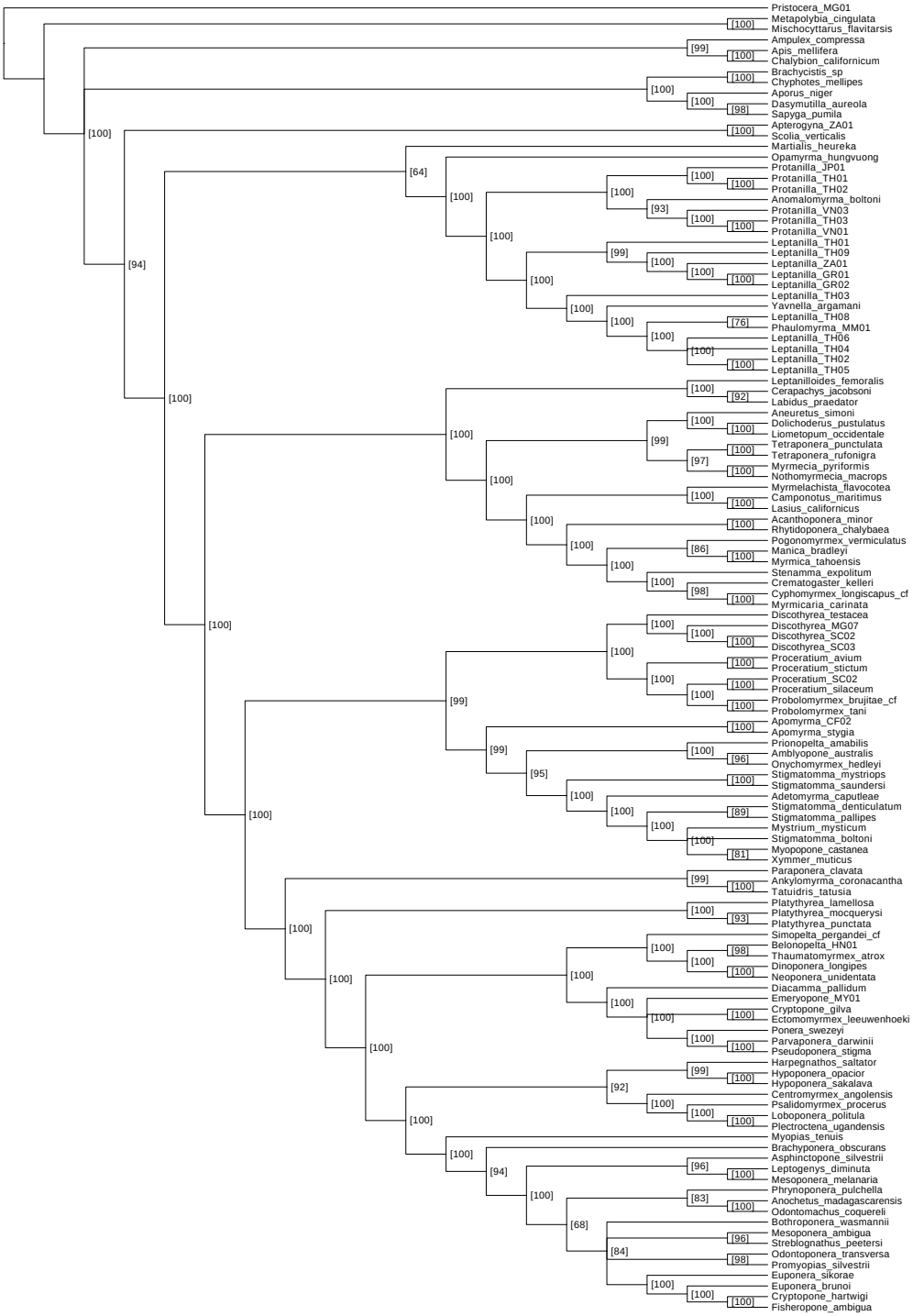

Supplementary Figure 19: Majority-rule consensus of maximum-likelihood trees inferred from 100 simulated alignments imitating third codon positions.

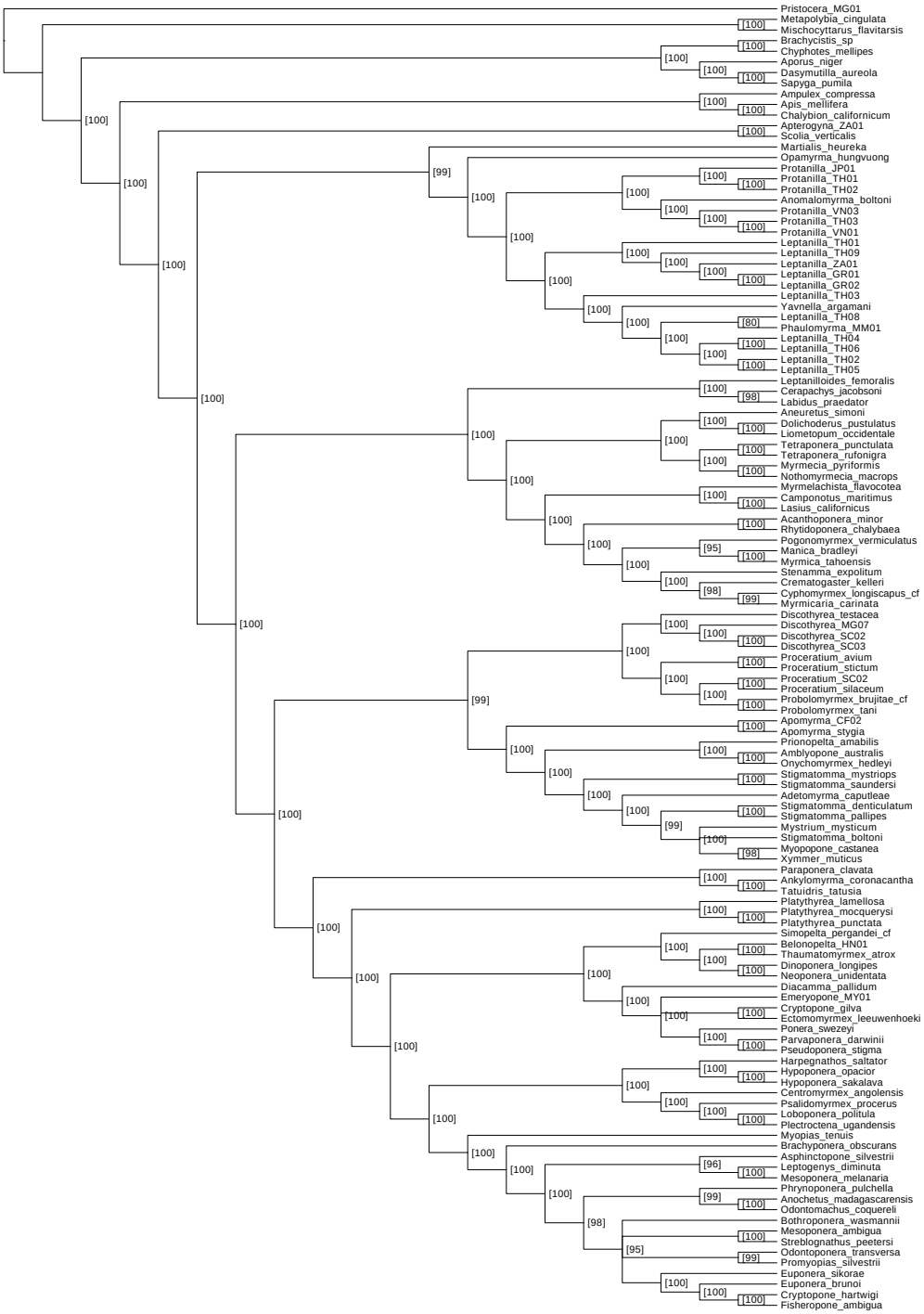

Supplementary Figure 20: Majority-rule consensus of maximum-likelihood trees inferred from 100 simulated alignments imitating first, second, and third codon positions combined.

Supplementary Table 1: Taxon properties in the full data set. AT and GC contents are expressed as proportions and nucleotide and gap columns contain character counts. Alignment has 7,451 sites total.

Taxon name	AT content	GC content	A	C	G	T	Gap
Acanthoponera minor	0.446	0.554	1792	2043	1967	1431	217
Adetomyrma caputleae	0.455	0.545	1822	2005	1933	1460	231
Amblyopone australis	0.452	0.548	1819	2008	1954	1448	222
Ampulex compressa	0.440	0.560	1790	2074	1958	1380	249
Aneuretus simoni	0.424	0.576	1711	2112	2054	1360	214
Ankylomyrma coronacantha	0.463	0.537	1839	1939	1943	1511	219
Anochetus madagascarensis	0.449	0.551	1833	2041	1949	1421	207
Anomalomyrma boltoni	0.514	0.486	2023	1745	1765	1696	222
Apis mellifera	0.491	0.509	1956	1813	1865	1590	225
Apomyrma CF02	0.483	0.517	1917	1883	1857	1575	219
Apomyrma stygia	0.478	0.522	1904	1906	1865	1553	223
Aporus niger	0.436	0.564	1756	2060	2012	1397	226
Apterogyna ZA01	0.438	0.562	1739	2025	2020	1413	254
Asphinctopone silvestrii	0.447	0.553	1801	2028	1976	1433	213
Belonopelta HN01	0.416	0.584	1686	2158	2072	1324	205
Bothroponera wasmannii	0.453	0.547	1833	2011	1944	1447	216
Brachycistis sp	0.502	0.498	2006	1781	1806	1614	204
Brachyponera obscurans	0.438	0.562	1781	2089	1983	1390	207
Camponotus maritimus	0.459	0.541	1823	1975	1925	1492	236
Centromyrmex angolensis	0.443	0.557	1773	2014	1998	1424	213
Cerapachys jacobsoni	0.452	0.548	1807	2002	1958	1464	220
Chalybion californicum	0.428	0.572	1753	2121	2015	1342	220
Chyphotes mellipes	0.452	0.548	1833	2021	1937	1428	232
Crematogaster kelleri	0.464	0.536	1843	1954	1923	1508	223
Cryptopone gilva	0.436	0.564	1766	2073	2013	1387	212
Cryptopone hartwigi	0.443	0.557	1791	2049	1968	1410	216
Cyphomyrmex longiscapus cf	0.469	0.531	1866	1934	1907	1530	214
Dasymutilla aureola	0.488	0.512	1965	1839	1854	1560	233
Diacamma pallidum	0.446	0.554	1801	2031	1982	1429	208
Dinoponera longipes	0.429	0.571	1723	2075	2051	1383	213
Discothyrea MG07	0.459	0.541	1856	1998	1914	1465	218
Discothyrea SC02	0.446	0.554	1802	2020	1988	1421	220
Discothyrea SC03	0.454	0.546	1835	2001	1947	1448	219
Discothyrea testacea	0.424	0.576	1737	2126	2048	1332	208
Dolichoderus pustulatus	0.456	0.544	1807	1982	1954	1488	217
Ectomomyrmex leeuwenhoeki	0.436	0.564	1764	2082	1999	1387	219
Emeryopone MY01	0.428	0.572	1748	2116	2029	1359	199
Euponera brunoi	0.441	0.559	1784	2065	1979	1410	207
Euponera sikorae	0.444	0.556	1797	2057	1966	1415	210
Fisheropone ambigua	0.444	0.556	1803	2054	1968	1413	213
Fulakora mystriops	0.491	0.509	1921	1824	1843	1620	243
Fulakora saundersi	0.454	0.546	1824	2002	1951	1467	207
Harpegnathos saltator	0.451	0.549	1815	2002	1973	1451	210
Hypoponera opacior	0.453	0.547	1799	1979	1978	1476	219
Hypoponera sakalava	0.450	0.550	1808	2006	1967	1445	219
Labidus praedator	0.463	0.537	1823	1951	1932	1525	219
Lasius californicus	0.452	0.548	1791	2012	1947	1478	223
Leptanilla GR01	0.528	0.472	2064	1698	1709	1741	239
Leptanilla GR02	0.529	0.471	2074	1692	1707	1740	238
Leptanilla TH01	0.515	0.485	2011	1732	1761	1704	243
Leptanilla TH02	0.506	0.494	1989	1775	1788	1659	240
Leptanilla TH03	0.512	0.488	2014	1742	1782	1684	229
Leptanilla TH04	0.505	0.495	1990	1783	1786	1652	240
Leptanilla TH05	0.508	0.492	1985	1757	1791	1679	239
Leptanilla TH06	0.504	0.496	1987	1786	1791	1650	237
Leptanilla TH08	0.506	0.494	1990	1779	1789	1663	230
Leptanilla TH09	0.532	0.468	2064	1661	1716	1776	234
Leptanilla ZA01	0.533	0.467	2079	1678	1689	1769	236
Leptanilloides femoralis	0.424	0.576	1730	2146	2021	1343	211
Leptogenys diminuta	0.454	0.546	1811	1997	1953	1480	210
Liometopum occidentale	0.442	0.558	1763	2043	1988	1432	225
Loboponera politula	0.431	0.569	1741	2078	2037	1379	216

Supplementary Table 1: Continued. Taxon properties in the full data set. AT and GC contents are expressed as proportions and nucleotide and gap columns contain character counts. Alignment has 7,451 sites total.

Taxon name	AT content	GC content	A	C	G	T	Gap
Manica bradleyi	0.440	0.560	1766	2060	1990	1415	219
Martialis heureka	0.466	0.534	1849	1960	1901	1520	221
Mesoponera ambigua	0.444	0.556	1792	2047	1973	1420	219
Mesoponera melanaria	0.455	0.545	1846	2013	1924	1440	222
Metapolybia cingulata	0.516	0.484	2022	1781	1745	1738	165
Mischocyttarus flavitarsis	0.530	0.470	2095	1718	1701	1757	180
Myopias tenuis	0.421	0.579	1703	2138	2055	1340	209
Myopopone castanea	0.471	0.529	1877	1935	1883	1525	231
Myrmecia pyriformis	0.464	0.536	1851	1971	1902	1500	227
Myrmelachista flavocotea	0.451	0.549	1784	2001	1961	1474	231
Myrmica tahoensis	0.438	0.562	1762	2062	1997	1406	223
Myrmicaria carinata	0.457	0.543	1821	1986	1942	1483	219
Mystrium voeltzkowi	0.476	0.524	1902	1915	1865	1535	234
Neoponera unidentata	0.443	0.557	1787	2042	1988	1420	199
Nothomyrmecia macrops	0.451	0.549	1811	2035	1935	1446	224
Odontomachus coquereli	0.445	0.555	1787	2029	1989	1436	204
Odontoponera transversa	0.456	0.544	1829	1989	1946	1464	216
Onychomyrmex hedleyi	0.463	0.537	1850	1961	1923	1495	222
Opamyrma hungvuong	0.473	0.527	1887	1935	1874	1535	220
Paraponera clavata	0.472	0.528	1873	1922	1896	1538	222
Parvaponera darwinii	0.416	0.584	1706	2173	2056	1308	208
Phaulomyrma MM01	0.507	0.493	2000	1775	1781	1661	234
Phrynoponera pulchella	0.440	0.560	1783	2062	1992	1406	207
Platythyrea lamellosa	0.460	0.540	1816	1975	1934	1516	210
Platythyrea mocquerysi	0.443	0.557	1792	2053	1977	1418	211
Platythyrea punctata	0.466	0.534	1837	1968	1896	1530	220
Plectroctena ugandensis	0.445	0.555	1791	2025	1986	1426	216
Pogonomyrmex vermiculatus	0.465	0.535	1857	1963	1903	1507	219
Ponera swezeyi	0.440	0.560	1766	2049	2007	1416	213
Prionopelta amabilis	0.481	0.519	1903	1894	1857	1569	228
Pristocera MG01	0.468	0.532	1863	1923	1907	1512	228
Probolomyrmex brujitae cf	0.413	0.587	1673	2151	2094	1309	224
Probolomyrmex tani	0.444	0.556	1777	2034	1979	1427	234
Proceratium avium	0.443	0.557	1787	2041	1979	1412	215
Proceratium SC02	0.461	0.539	1836	1957	1941	1501	216
Proceratium silaceum	0.458	0.542	1834	1968	1950	1483	216
Proceratium stictum	0.447	0.553	1794	2024	1971	1430	215
Promyopias silvestrii	0.457	0.543	1839	1985	1923	1456	219
Protanilla JP01	0.499	0.501	1964	1817	1798	1643	229
Protanilla TH01	0.517	0.483	2038	1768	1718	1699	228
Protanilla TH02	0.518	0.482	2037	1759	1724	1703	228
Protanilla TH03	0.490	0.510	1946	1861	1836	1604	204
Protanilla VN01	0.491	0.509	1941	1849	1836	1615	210
Protanilla VN03	0.491	0.509	1943	1853	1832	1607	214
Psalidomyrmex procerus	0.436	0.564	1776	2078	2005	1383	209
Pseudoponera stigma	0.419	0.581	1704	2138	2066	1324	219
Rhytidoponera chalybaea	0.452	0.548	1814	2005	1961	1458	213
Sapyga pumila	0.407	0.593	1689	2193	2105	1257	205
Scolia verticalis	0.484	0.516	1939	1894	1833	1554	231
Simopelta pergandei cf	0.441	0.559	1777	2058	1998	1422	196
Stenamma expolitum	0.451	0.549	1787	1981	1979	1466	237
Stigmatomma boltoni	0.474	0.526	1884	1926	1869	1535	237
Stigmatomma denticulatum	0.454	0.546	1826	2007	1938	1455	225
Stigmatomma pallipes	0.456	0.544	1833	1997	1930	1460	231
Streblognathus peetersi	0.438	0.562	1768	2074	1997	1399	213
Tatuidris tatusia	0.478	0.522	1886	1888	1879	1559	239
Tetraponera punctulata	0.434	0.566	1729	2064	2017	1401	240
Tetraponera rufonigra	0.448	0.552	1788	2021	1961	1440	241
Thaumatomyrmex atrox	0.438	0.562	1752	2054	2010	1415	214
Xymmer muticus	0.472	0.528	1871	1925	1891	1538	225
Yavnella argamani	0.511	0.489	1993	1754	1775	1688	241

Supplementary Table 2: Results of compositional homogeneity tests for all data partitions. P-values below 0.05 considered significant violation of homogeneity assumption.

Partition	Corrected test p-value	Chi-squared p-value
Full data set	0.000	0.000
28S	0.000	1.000
abdA	0.000	0.990
abdA 1st pos	0.905	1.000
abdA 2nd pos	0.262	1.000
abdA 3rd pos	0.000	0.000
argK	0.000	0.000
argK 1st pos	0.698	1.000
argK 2nd pos	0.987	1.000
argK 3rd pos	0.000	0.000
Antp	0.000	0.000
Antp 1st pos	0.847	1.000
Antp 2nd pos	0.520	1.000
Antp 3rd pos	0.000	0.000
EF1aF2	0.000	0.000
EF1aF2 1st pos	1.000	1.000
EF1aF2 2nd pos	0.555	1.000
EF1aF2 3rd pos	0.000	0.000
LW Rh	0.000	0.000
LW Rh 1st pos	1.000	1.000
LW Rh 2nd pos	0.926	1.000
LW Rh 3rd pos	0.000	0.000
NaK	0.000	0.025
NaK 1st pos	0.558	1.000
NaK 2nd pos	0.460	1.000
NaK 3rd pos	0.000	0.000
POLD1	0.000	0.000
POLD1 1st pos	0.004	1.000
POLD1 2nd pos	0.766	1.000
POLD1 3rd pos	0.000	0.000
Top 1	0.000	0.000
Top 1 1st pos	0.106	1.000
Top 1 2nd pos	0.964	1.000
Top 1 3rd pos	0.000	0.000
Ubx	0.000	0.009
Ubx 1st pos	0.038	1.000
Ubx 2nd pos	0.202	1.000
Ubx 3rd pos	0.000	0.000
Wg	0.000	0.000
Wg 1st pos	0.749	1.000
Wg 2nd pos	0.923	1.000
Wg 3rd pos	0.000	0.000
All 1st pos	0.028	1.000
All 2nd pos	1.000	1.000
All 3rd pos	0.000	0.000

Supplementary Table 3: Calibration fossils used in divergence dating analysis.

Fossil genus	Fossil species	Least inclusive clade (total group)	Least inclusive clade (total group) in this study	Deposit	Age	Reference(s)	Notes
Pristomyrmex	*rasnitsyni*	*Pristomyrmex*	*Crematogaster*	Danish amber	36	*Pristomyrmex* in late Eocene Danish amber (Dlussky and Radchenko, 2011).	Node calibration in Ward et al. (2015): 42 (offset), 52 (median), 73 (95% quantile)
Aphaenogaster	*antiqua*	*Aphaenogaster* sensu stricto	Stenamma	Rovno amber	36	*Aphaenogaster antiqua* from Rovno amber (Dlussky and Perkovsky, 2002).	Node calibration in Ward et al. (2015): 42 (offset), 52 (median), 73 (95% quantile)
Myrmica	*longispinosa*	*Myrmica*	*Myrmica*	Baltic amber	36	Four *Myrmica* species (*longispinosa*, *rudis*, *intermedia*, *eocenica*) from Baltic amber (Dlussky and Rasnitsyn, 2009), not definitely assignable to modern species groups, although similar to the plesiotypic *ritae*-group (Radchenko et al., 2007).	Node calibration in Ward et al. (2015): 42 (offset), 60 (median), 85 (95% quantile)
Gnamptogenys	*europaea*	*Gnamptogenys*	*Rhytidoponera*	Baltic amber	36	Two species of *Gnamptogenys* in Baltic amber (Dlussky, 2009).	
Kyromyrma	*neffi*	Formicinae	*Myrmelachista* plus *Camponotus* plus *Lasius*	New Jersey amber	92	*Kyromyrma* in New Jersey amber (Grimaldi and Agosti, 2000).	Node calibration in Ward et al. (2015): 92 (offset), 95 (median), 120 (95% quantile)
Lasius	*glom*	*Lasius*	*Lasius*	Kishenehn Formation	46	*Lasius glom* in Kishenehn Formation (Lapolla and Greenwalt, 2015)	
Oecophylla	*longiceps*	*Oecophylla*	*Camponotus*	Grube Messel, Germany	47	*Oecophylla longiceps* from Grube Messel, Darmstadt, Germany; middle Eocene, Lutetian (ca. 47 Ma) (Dlussky et al., 2008).	
Tetraponera	sp Oise	*Tetraponera*	*Tetraponera*	Oise amber	52	Three species of *Tetraponera* in Oise amber (Aria et al. (2011); Aria pers. comm.).	Node calibration in Chomicki et al. (2015) of crown Pseudomyrmecinae with truncated normal prior, mean 55, sd 5; truncated at 55 Ma.
Tetraponera	*simplex*	*Tetraponera* crown	*Tetraponera punctulata*	Baltic amber	36	*Tetraponera simplex* in Baltic amber (Dlussky and Rasnitsyn, 2009), with some features of *T. nigra* group.	Considered crown *Tetraponera*, given mandible structure (reduced teeth) and loss of ocelli.
Ypresiomyrma	*rebekkae*	Myrmeciinae	*Myrmecia* plus *Nothomyrmecia*	Mo-Clay, Denmark	53.5	*Ypresiomyrma rebekkae* from Mo-clay, Stolleklint, Isle of Fur, Denmark; Eocene, Ypresian (Rust and Andersen (1999); Archibald et al. (2006); Dlussky et al. (2015)).	
Prionomyrmex	*janzeni*	*Nothomyrmecia*	*Nothomyrmecia*	Baltic amber	36	Two species of *Prionomyrmex* in Baltic amber (Mayr, 1868; Baroni Urbani, 2000).	
Dolichoderus	*kohlsi*	*Dolichoderus*	*Dolichoderus*	Green River Formation	51.5	*Dolichoderus kohlsi* from Green River Formation (Dlussky and Rasnitsyn, 2003).	Second most abundant species of ant in Green River Formation.
Liometopum	*oligocenicum*	*Liometopum*	*Liometopum*	Baltic amber	36	*Liometopum oligocenicum* in Baltic amber (Dlussky, 1997), but rare (Dlussky and Rasnitsyn, 2009).	Node calibration in Ward et al. (2010) (ame calibration for *Liometopum* and *Tapinoma*): 42 (offset), 54 (median), 70 (95% quantile); in Boudinot et al. (2016): 42, 59, 77.
Chronomyrmex	*medicinehatensis*	Dolichoderinae	*Dolichoderus* plus *Liometopum*	Canadian Grassy Lake amber	78	*Chronomyrmex* in Grassy Lake amber (McKellar et al. (2013); Boudinot et al. (2016)).	Node calibration in Boudinot et al. (2016): 78 (offset), 95 (median), 110 (95% quantile).
Aneuretellus	*deformis*	Aneuretinae plus Dolichoderinae	Aneuretinae plus Dolichoderinae	Sakhalin amber	57.5	*Aneuretellus deformis* from Sakhalin amber (Dlussky, 1988).	Because of possible paraphyly of Aneuretinae we assume a conservative assignment to the total group of (Aneuretinae plus Dolichoderinae), i.e. crown dolichoderomorphs.
Procerapachys	*favosus*	Dorylinae	*Labidus* plus *Cerapachys* plus *Leptanilloides*	Baltic amber	36	Three species of *Procerapachys* in Baltic amber (Dlussky, 2009).	Node calibration in (Brady et al., 2014): 42 (offset), 80 (median), 100 (95% quantile)
Platythyrea	*dlusskyi*	*Platythyrea*	*Platythyrea*	Oise amber	52	*Platythyrea dlusskyi* in Oise amber (Aria et al., 2011).	Different calibration (Baltic amber) in Ward et al. (2015).
Hypoponera	*atavia*	*Hypoponera*	*Hypoponera*	Baltic amber	36	*Hypoponera atavia* in Baltic amber (Dlussky, 1997; Dlussky and Rasnitsyn, 2009).	
Odontomachus	*paleomyagra*	*Odontomachus*	*Odontomachus*	Bilina, Czech Republic	18	*Odontomachus paleomyagra* from Bilina, Czech Republic; Early Miocene (Burdigalian, 16-20 Ma) (Wappler et al., 2014).	
Anochetus	*lucidus*	*Anochetus*	*Anochetus*	Dominican amber	17	*Anochetus* in Dominican amber (Urbani, 1980; Andrade, 1994; MacKay, 1991).	
Ponera	*mayri*	*Ponera*	*Ponera swezeyi*	Baltic amber	36	Dlussky and Rasnitsyn (2009) recognizes three *Ponera* species from Baltic amber.	
Stigmatomma	*groehni*	*Stigmatomma denticulatum* group	*Stigmatomma denticulatum*	Baltic amber	36	*Stigmatomma groehni* in Baltic amber, said to be member of *S. denticulatum* group (Dlussky, 2009).	Node calibration in Ward and Fisher (2016): 42 (offset), 55 (median), 80 (95% quantile)
Stigmatomma	*electrina*	*Stigmatomma* (XMMAS clade)	*Stigmatomma mystriops*	Baltic amber	36	*Stigmatomma electrina* (male) in Baltic amber (Dlussky, 2009).	
Prionopelta	sp Dominican	*Prionopelta*	*Prionopelta*	Dominican amber	17	Undescribed *Prionopelta* species from Dominican amber (Wilson, 2004).	Node calibration in Ward and Fisher (2016): 15 (offset), 40 (median), 60 (95% quantile)
Bradoponera	*electrina*	Proceratiinae	*Discothyrea* plus *Proceratium* plus *Probolomyrmex*	Baltic amber	36	Three species of *Bradoponera* in Baltic amber (Urbani and Andrade, 2003)	
Proceratium	*eocenicum*	*Proceratium*	*Proceratium* plus *Probolomyrmex*	Baltic amber	36	*Proceratium eocenicum* in Baltic amber (Dlussky, 2009).	
Agroecomyrmex	*duisburgi*	*Tatuidris*	*Tatuidris*	Baltic amber	36	*Agroecomyrmex duisburgi* (Agroecomyrmecinae) in Baltic amber (Wheeler, 1915; Dlussky and Rasnitsyn, 2009).	Node calibration in Ward et al. (2015): 42 (offset), 60 (median), 90 (95% quantile)
Camelomecia	*janovitzi*	Formicidae	Formicidae	Myanmar amber	97	(Barden and Grimaldi, 2016).	
Gerontoformica	*cretacica*	Formicidae	Formicidae	Charentese amber	99.5	*Gerontoformica cretacica* and *G. occidentalis* in Charentese amber (Perrichot et al., 2008; Perrichot, 2015; Barden and Grimaldi, 2016).	*Sphecomyrmodes* now considered a junior synonym (Barden and Grimaldi, 2016).
Pompilopterus	*difficilis*	Apoidea	Apoidea	Lulworth Formation, England	143	*Pompilopterus difficilis* (Rasnitsyn and Jarzembowski, 1998).	Age range: 145.5 to 140.2 Ma.
Architiphia	*rasnitsyni*	Anthoboscinae	*Chyphotes*	Crato formation, Ceará, Brazil	117.6	Darling and Sharkey (1990). Date from fossilworks (midpoint of 122.46 to 112.6)	Said to be Anthoboscinae. Note that anthoboscines are Thynnidae, not Tiphiidae (sensu Pilgrim et al. (2008)).
Thanatotiphia	*nyx*	Tiphioidea plus Thynnoidea	*Chyphotes* plus *Brachycistis*	Myanmar amber	97	Engel et al. (2009). Date from fossilworks (midpoint of 99.7 to 94.3).	Not definitively assigned to thynnid or tiphiid (s.s.) groups.
Eorhopalosoma	*gorgyra*	Rhopalosomatidae	*Metapolybia* plus *Mischocyttarus*	Myanmar amber	97	Engel (2008). Date from fossilworks (midpoint of 99.7 to 94.3).	Engel (2008) argues that this is a crown rhopalosomatid.
Mesorhopalo-soma	*cearae*	Rhopalosomatidae	*Metapolybia* plus *Mischocyttarus*	Crato formation, Ceará, Brazil	117.6	Darling and Sharkey (1990). Date from fossilworks (midpoint of 122.46 to 112.6).	*Mesorhopalosoma* likely a stem rhopalosomatid.
Paleogenia	*wahisi*	Pepsinae	*Aporus*	Baltic amber	36	Rodriguez et al. (2016). Note that these authors remove *Bryopompilus* (Myanmar amber) from Pompilidae.	
Cretosapyga	*resinicola*	Sapygidae	*Sapyga*	Myanmar amber	97	Bennett and Engel (2005)). Date from fossilworks (midpoint of 99.7 to 94.3).	
Protomutilla	*archaeotricho-soma*	Myrmosidae	*Dasymutilla*	Baltic amber	36	Lelej (1986), Brothers (1974).	
Cretoscolia	*conquensis*	Scoliidae	*Scolia*	Barremian, Spain	127.7	Rasnitsyn and Martínez-Delclòs (2000). Date from fossilworks (midpopint of 130.0 to 125.45).	At least seven other species of *Cretoscolia* have been described, all from the Cretaceous.
Cariridris	*bipetiolata*	Ampulicidae	*Ampulex*	Crato formation, Ceará, Brazil	117.6	Ohl (2004). Date from fossilworks (midpoint of 122.46 to 112.6)	
Cretampulex	*gracilis*	Ampulicidae	*Ampulex*	Myanmar amber	97	Antropov (2000). Date from fossilworks (midpoint of 99.7 to 94.3).	
Cretospilomena	*familiaris*	Pemphredoninae	*Apis*	Myanmar amber	97	Antropov (2000, 2011). Date from fossilworks (midpoint of 99.7 to 94.3).	There are many other Cretaceous pemphredonines.
Melittosphex	*burmensis*	Anthophila	*Apis*	Myanmar amber	97	Poinar and Danforth (2006), Poinar (2009). Date from fossilworks (midpoint of 99.7 to 94.3).	

Supplementary Table 4: Taxa included in the study with GenBank accession numbers and specimen voucher information. Detailed collection data for each species is available by searching for the specimen code on AntWeb (www.antweb.org).

Taxon	Voucher	28S	Wg	AA	LR	F2	ArgK	Top1	Ubx	DP	NK	AP
Acanthoponera minor	CASENT0039772	EF012953	EF013661	EF013081	EF013533	EF013371	KJ861140	KJ861751	KJ860480	XXXXXXXX	XXXXXXXX	XXXXXXXX
Adetomyrma caputleae	CASENT0491481	EF012956	EF013664	EF013084	EF013536	EF013375	KU671604	KU671667	KU671730	KU671870	KU671947	KU671793
Amblyopone australis	CASENT0106229	KJ860056	KJ861944	KJ861331	KJ861515	KJ859868	KJ861141	KJ861752	KJ860481	KU671871	KU671948	KU671794
Aneuretus simoni	CASENT0007014	EF012961	EF013669	EF013089	EF013541	EF013382	FJ939840	KJ523645	KJ523562	XXXXXXXX	XXXXXXXX	XXXXXXXX
Ankylomyrma coronacantha	CASENT0406734	KJ860057	KJ861945	KJ861332	KJ861516	KJ859869	KJ861142	KJ861753	KJ860482	KU671924	KU672001	KU671847
Anochetus madagascarensis	CASENT0498593	EF012962	EF013670	EF013090	EF013542	EF013383	XXXXXXXX	XXXXXXXX	XXXXXXXX	XXXXXXXX	XXXXXXXX	XXXXXXXX
Anomalomyrma boltoni	CASENT0217032	KU671445	KU671598	KU672069	KU671547	KU671496	KU671656	KU671719	KU671782	KU671925	KU672002	KU671848
Apomyrma CF02	CASENT0086073	KU671402	KU671555	KU672026	KU671504	KU671453	KU671607	KU671670	KU671733	KU671874	KU671951	KU671797
Apomyrma stygia	CASENT0007017	EF012967	EF013675	EF013095	EF013547	EF013390	KU671608	KU671671	KU671734	KU671875	KU671952	KU671798
Asphinctopone silvestrii	CASENT0417123	XXXXXXXX	XXXXXXXX	XXXXXXXX	XXXXXXXX	XXXXXXXX	XXXXXXXX	XXXXXXXX	XXXXXXXX	XXXXXXXX	XXXXXXXX	XXXXXXXX
Belonopelta HN01	CASENT0235904	XXXXXXXX	XXXXXXXX	XXXXXXXX	XXXXXXXX	XXXXXXXX	XXXXXXXX	XXXXXXXX	XXXXXXXX	XXXXXXXX	XXXXXXXX	XXXXXXXX
Bothroponera wasmannii	CASENT0076787	XXXXXXXX	XXXXXXXX	XXXXXXXX	XXXXXXXX	XXXXXXXX	XXXXXXXX	XXXXXXXX	XXXXXXXX	XXXXXXXX	XXXXXXXX	XXXXXXXX
Brachyponera obscurans	CASENT0059658	XXXXXXXX	XXXXXXXX	XXXXXXXX	XXXXXXXX	XXXXXXXX	XXXXXXXX	XXXXXXXX	XXXXXXXX	XXXXXXXX	XXXXXXXX	XXXXXXXX
Camponotus maritimus	CASENT0106083	AY867464	AY867433	AY867480	AY867495	EF013400	KT443562	KT443642	KT443722	XXXXXXXX	XXXXXXXX	XXXXXXXX
Centromyrmex angolensis	CASENT0417147	EF012979	EF013687	EF013107	EF013559	EF013403	XXXXXXXX	XXXXXXXX	XXXXXXXX	XXXXXXXX	XXXXXXXX	XXXXXXXX
Cerapachys jacobsoni	CASENT0106233	KJ523194	KJ523510	KJ523841	KJ523731	KJ523786	KJ523310	KJ523655	KJ523572	KU671927	KU672004	KU671850
Crematogaster kelleri	CASENT0498885	KJ859905	KJ861793	KJ861182	KJ861367	KJ859719	KJ860961	KJ861563	KJ860292	XXXXXXXX	XXXXXXXX	XXXXXXXX
Cryptopone gilva	CASENT0106309	XXXXXXXX	XXXXXXXX	XXXXXXXX	XXXXXXXX	XXXXXXXX	XXXXXXXX	XXXXXXXX	XXXXXXXX	XXXXXXXX	XXXXXXXX	XXXXXXXX
Cryptopone hartwigi	CASENT0217039	XXXXXXXX	XXXXXXXX	XXXXXXXX	XXXXXXXX	XXXXXXXX	XXXXXXXX	XXXXXXXX	XXXXXXXX	XXXXXXXX	XXXXXXXX	XXXXXXXX
Cyphomyrmex longiscapus cf	CASENT0052777	KJ859911	KJ861799	KJ861187	KJ861372	KJ859724	KJ860967	KJ861569	KJ860298	XXXXXXXX	XXXXXXXX	XXXXXXXX
Diacamma pallidum	CASENT0106139	XXXXXXXX	XXXXXXXX	XXXXXXXX	XXXXXXXX	XXXXXXXX	XXXXXXXX	XXXXXXXX	XXXXXXXX	XXXXXXXX	XXXXXXXX	XXXXXXXX
Dinoponera longipes	CASENT0004663	XXXXXXXX	XXXXXXXX	XXXXXXXX	XXXXXXXX	XXXXXXXX	XXXXXXXX	XXXXXXXX	XXXXXXXX	XXXXXXXX	XXXXXXXX	XXXXXXXX
Discothyrea MG07	CASENT0042927	EF012987	EF013695	EF013115	EF013567	EF013415	XXXXXXXX	XXXXXXXX	XXXXXXXX	XXXXXXXX	XXXXXXXX	XXXXXXXX
Discothyrea SC02	CASENT0159387	XXXXXXXX	XXXXXXXX	XXXXXXXX	XXXXXXXX	XXXXXXXX	XXXXXXXX	XXXXXXXX	XXXXXXXX	XXXXXXXX	XXXXXXXX	XXXXXXXX
Discothyrea SC03	CASENT0161605	XXXXXXXX	XXXXXXXX	XXXXXXXX	XXXXXXXX	XXXXXXXX	XXXXXXXX	XXXXXXXX	XXXXXXXX	XXXXXXXX	XXXXXXXX	XXXXXXXX
Discothyrea testacea	CASENT0270725	KU671446	KU671599	KU672070	KU671548	KU671497	KU671658	KU671721	KU671784	KU671929	KU672006	KU671852
Dolichoderus pustulatus	CASENT0106164	FJ939792	FJ940028	FJ939824	FJ939995	FJ939963	FJ939859	KJ523685	KJ523602	KU671930	KU672007	KU671853
Ectomomyrmex leeuwenhoeki	CASENT0106306	XXXXXXXX	XXXXXXXX	XXXXXXXX	XXXXXXXX	XXXXXXXX	XXXXXXXX	XXXXXXXX	XXXXXXXX	XXXXXXXX	XXXXXXXX	XXXXXXXX
Emeryopone MY01	CASENT0226984	XXXXXXXX	XXXXXXXX	XXXXXXXX	XXXXXXXX	XXXXXXXX	XXXXXXXX	XXXXXXXX	XXXXXXXX	XXXXXXXX	XXXXXXXX	XXXXXXXX
Euponera brunoi	CASENT0297649	XXXXXXXX	XXXXXXXX	XXXXXXXX	XXXXXXXX	XXXXXXXX	XXXXXXXX	XXXXXXXX	XXXXXXXX	XXXXXXXX	XXXXXXXX	XXXXXXXX
Euponera sikorae	CASENT0487847	EF013032	EF013740	EF013160	EF013612	EF013475	XXXXXXXX	XXXXXXXX	XXXXXXXX	XXXXXXXX	XXXXXXXX	XXXXXXXX
Fisheropone ambigua	CASENT0289205	XXXXXXXX	XXXXXXXX	XXXXXXXX	XXXXXXXX	XXXXXXXX	XXXXXXXX	XXXXXXXX	XXXXXXXX	XXXXXXXX	XXXXXXXX	XXXXXXXX
Harpegnathos saltator	CASENT0179535	XXXXXXXX	XXXXXXXX	XXXXXXXX	XXXXXXXX	XXXXXXXX	XXXXXXXX	XXXXXXXX	XXXXXXXX	XXXXXXXX	XXXXXXXX	XXXXXXXX
Hypoponera opacior	CASENT0106093	AY703555	AY703622	AY703689	AY703756	EF013428	KU671659	KU671722	KU671785	KU671931	KU672008	KU671854
Hypoponera sakalava	CASENT0494141	EF012997	EF013705	EF013125	EF013577	EF013429	XXXXXXXX	XXXXXXXX	XXXXXXXX	XXXXXXXX	XXXXXXXX	XXXXXXXX
Labidus praedator	CASENT0106227	KJ523222	KJ523538	KJ523869	KJ523759	KJ523814	KJ523345	KJ523691	KJ523608	XXXXXXXX	XXXXXXXX	XXXXXXXX
Lasius californicus	CASENT0106045	EF012998	EF013706	EF013126	EF013578	EF013430	KJ523346	KJ523692	KJ523609	KU671932	KU672009	KU671855
Leptanilla GR01	CASENT0106236	EF012999	EF013707	JN967846	JN967889	JN967829	JN967880	JN967820	JN967809	XXXXXXXX	XXXXXXXX	XXXXXXXX
Leptanilla GR02	CASENT0106067	JN967864	JN967856	JN967848	JN967891	JN967831	JN967883	JN967823	JN967812	XXXXXXXX	XXXXXXXX	XXXXXXXX
Leptanilla TH01	CASENT0119792	KU671447	KU671600	KU672071	KU671549	KU671498	KU671660	KU671723	KU671786	KU671933	KU672010	KU671856
Leptanilla TH02	CASENT0119531	XXXXXXXX	XXXXXXXX	XXXXXXXX	XXXXXXXX	XXXXXXXX	XXXXXXXX	XXXXXXXX	XXXXXXXX	XXXXXXXX	XXXXXXXX	XXXXXXXX
Leptanilla TH03	CASENT0129721	XXXXXXXX	XXXXXXXX	XXXXXXXX	XXXXXXXX	XXXXXXXX	XXXXXXXX	XXXXXXXX	XXXXXXXX	XXXXXXXX	XXXXXXXX	XXXXXXXX
Leptanilla TH04	CASENT0129695	XXXXXXXX	XXXXXXXX	XXXXXXXX	XXXXXXXX	XXXXXXXX	XXXXXXXX	XXXXXXXX	XXXXXXXX	XXXXXXXX	XXXXXXXX	XXXXXXXX
Leptanilla TH05	CASENT0134656	XXXXXXXX	XXXXXXXX	XXXXXXXX	XXXXXXXX	XXXXXXXX	XXXXXXXX	XXXXXXXX	XXXXXXXX	XXXXXXXX	XXXXXXXX	XXXXXXXX
Leptanilla TH06	CASENT0129609	XXXXXXXX	XXXXXXXX	XXXXXXXX	XXXXXXXX	XXXXXXXX	XXXXXXXX	XXXXXXXX	XXXXXXXX	XXXXXXXX	XXXXXXXX	XXXXXXXX
Leptanilla TH08	CASENT0227555	XXXXXXXX	XXXXXXXX	XXXXXXXX	XXXXXXXX	XXXXXXXX	XXXXXXXX	XXXXXXXX	XXXXXXXX	XXXXXXXX	XXXXXXXX	XXXXXXXX
Leptanilla TH09	CASENT0227556	XXXXXXXX	XXXXXXXX	XXXXXXXX	XXXXXXXX	XXXXXXXX	XXXXXXXX	XXXXXXXX	XXXXXXXX	XXXXXXXX	XXXXXXXX	XXXXXXXX
Leptanilla ZA01	CASENT0106085	AY867452	AY867421	AY867468	AY867483	EF013432	XXXXXXXX	XXXXXXXX	XXXXXXXX	XXXXXXXX	XXXXXXXX	XXXXXXXX
Leptanilloides femoralis	CASENT0106180	KJ523223	KJ523539	KJ523870	KJ523760	KJ523815	KJ523347	KJ523693	KJ523610	XXXXXXXX	XXXXXXXX	XXXXXXXX
Leptogenys diminuta	CASENT0106010	EF013000	EF013708	EF013128	EF013580	EF013435	XXXXXXXX	XXXXXXXX	XXXXXXXX	XXXXXXXX	XXXXXXXX	XXXXXXXX
Liometopum occidentale	CASENT0106078	AY867465	AY867434	AY867481	AY867496	EF013441	FJ939875	XXXXXXXX	XXXXXXXX	XXXXXXXX	XXXXXXXX	XXXXXXXX
Lobopone politula	CASENT0003095	EF013005	EF013713	EF013133	EF013585	EF013442	XXXXXXXX	XXXXXXXX	XXXXXXXX	XXXXXXXX	XXXXXXXX	XXXXXXXX
Manica bradleyi	CASENT0106022	EF013006	EF013714	EF013134	EF013586	EF013443	FJ939877	KJ523698	KJ523615	KU671934	KU672011	KU671857
Martialis heureka	CASENT0106181	KU671448	KU671601	KU672072	KU671550	KU671499	KU671661	KU671724	KU671787	KU671935	KU672012	KU671858
Mesoponera ambigua	CASENT0441714	XXXXXXXX	XXXXXXXX	XXXXXXXX	XXXXXXXX	XXXXXXXX	XXXXXXXX	XXXXXXXX	XXXXXXXX	XXXXXXXX	XXXXXXXX	XXXXXXXX
Mesoponera melanaria	CASENT0145371	XXXXXXXX	XXXXXXXX	XXXXXXXX	XXXXXXXX	XXXXXXXX	XXXXXXXX	XXXXXXXX	XXXXXXXX	XXXXXXXX	XXXXXXXX	XXXXXXXX
Myopias tenuis	CASENT0106254	XXXXXXXX	XXXXXXXX	XXXXXXXX	XXXXXXXX	XXXXXXXX	XXXXXXXX	XXXXXXXX	XXXXXXXX	XXXXXXXX	XXXXXXXX	XXXXXXXX
Myopopone castanea	CASENT0106147	KU671404	KU671557	KU672028	KU671506	KU671455	KU671611	KU671674	KU671737	KU671878	KU671955	KU671801
Myrmecia pyriformis	CASENT0106088	AY703567	AY703634	AY703701	AY703768	EF013454	FJ939878	KJ523699	KJ523616	KU671936	KU672013	KU671859
Myrmelachista flavocotea	CASENT0106049	EF013017	EF013725	EF013145	EF013597	EF013457	KJ861144	KJ861755	KJ860484	XXXXXXXX	XXXXXXXX	XXXXXXXX
Myrmica tahoensis	CASENT0106091	AY703562	AY703629	AY703696	AY703763	EF013459	GU085791	KJ861640	KJ860369	XXXXXXXX	XXXXXXXX	XXXXXXXX
Myrmicaria carinata	KJ859969	KJ861857	KJ861244	KJ861429	KJ859781	KJ861034	KJ861641	KJ860370	XXXXXXXX	XXXXXXXX	XXXXXXXX	XXXXXXXX
Mystrium voeltzkowi	CASENT0076622	EF013022	EF013730	EF013150	EF013602	EF013463	KU671613	KU671676	KU671739	KU671880	KU671957	KU671803
Neoponera unidentata	CASENT0106307	XXXXXXXX	XXXXXXXX	XXXXXXXX	XXXXXXXX	XXXXXXXX	XXXXXXXX	XXXXXXXX	XXXXXXXX	XXXXXXXX	XXXXXXXX	XXXXXXXX
Nothomyrmecia macrops	CASENT0106089	AY703568	AY703635	AY703702	AY703769	EF013466	FJ939880	KJ523703	KJ523620	XXXXXXXX	XXXXXXXX	XXXXXXXX
Odontomachus coquereli	CASENT0499525	EF013026	EF013734	EF013154	EF013606	EF013469	KU671662	KU671725	KU671788	KU671937	KU672014	KU671860
Odontoponera transversa	CASENT0010127	EF013027	EF013735	EF013155	EF013607	EF013470	XXXXXXXX	XXXXXXXX	XXXXXXXX	XXXXXXXX	XXXXXXXX	XXXXXXXX
Onychomyrmex hedleyi	CASENT0106018	EF013029	EF013737	EF013157	EF013609	EF013472	KU671615	KU671678	KU671741	KU671882	KU671959	KU671805
Opamyrma hungvuong	CASENT0178347	KU671407	KU671560	KU672031	KU671509	KU671458	KU671616	KU671679	KU671742	KU671883	KU671960	KU671806
Paraponera clavata	CASENT0106092	AY703556	AY703623	AY703690	AY703757	EF013477	KJ523355	KJ523704	KJ523621	KU671938	KU672015	KU671861
Parvaponera darwinii	CASENT0484950	XXXXXXXX	XXXXXXXX	XXXXXXXX	XXXXXXXX	XXXXXXXX	XXXXXXXX	XXXXXXXX	XXXXXXXX	XXXXXXXX	XXXXXXXX	XXXXXXXX
Phaulomyrma MM01	CASENT0179537	XXXXXXXX	XXXXXXXX	XXXXXXXX	XXXXXXXX	XXXXXXXX	XXXXXXXX	XXXXXXXX	XXXXXXXX	XXXXXXXX	XXXXXXXX	XXXXXXXX
Phrynoponera pulchella	CASENT0217034	XXXXXXXX	XXXXXXXX	XXXXXXXX	XXXXXXXX	XXXXXXXX	XXXXXXXX	XXXXXXXX	XXXXXXXX	XXXXXXXX	XXXXXXXX	XXXXXXXX
Platythyrea lamellosa	CASENT0106138	XXXXXXXX	XXXXXXXX	XXXXXXXX	XXXXXXXX	XXXXXXXX	XXXXXXXX	XXXXXXXX	XXXXXXXX	XXXXXXXX	XXXXXXXX	XXXXXXXX
Platythyrea mocquerysi	CASENT0106094	AY867453	AY867422	AY867469	AY867484	EF013484	KJ861145	KJ861756	KJ860485	KU671939	KU672016	KU671862
Platythyrea punctata	CASENT0006819	EF013040	EF013748	EF013168	EF013620	EF013485	XXXXXXXX	XXXXXXXX	XXXXXXXX	XXXXXXXX	XXXXXXXX	XXXXXXXX
Plectroctena ugandensis	CASENT0003063	EF013041	EF013749	EF013169	EF013621	EF013486	XXXXXXXX	XXXXXXXX	XXXXXXXX	XXXXXXXX	XXXXXXXX	XXXXXXXX
Pogonomyrmex vermiculatus	KJ859996	KJ861884	KJ861271	KJ861456	KJ859808	KJ861069	KJ861676	KJ860405	XXXXXXXX	XXXXXXXX	XXXXXXXX	XXXXXXXX
Ponera swezeyi	CASENT0047257	XXXXXXXX	XXXXXXXX	XXXXXXXX	XXXXXXXX	XXXXXXXX	XXXXXXXX	XXXXXXXX	XXXXXXXX	XXXXXXXX	XXXXXXXX	XXXXXXXX
Prionopelta amabilis	CASENT0052775	KU671409	KU671562	KU672033	KU671511	KU671460	KU671618	KU671681	KU671744	KU671885	KU671962	KU671808
Probolomyrmex brujitae cf	CASENT0106137	XXXXXXXX	XXXXXXXX	XXXXXXXX	XXXXXXXX	XXXXXXXX	XXXXXXXX	XXXXXXXX	XXXXXXXX	XXXXXXXX	XXXXXXXX	XXXXXXXX
Probolomyrmex tani	CASENT0041507	EF013050	EF013758	EF013178	EF013630	EF013495	XXXXXXXX	XXXXXXXX	XXXXXXXX	XXXXXXXX	XXXXXXXX	XXXXXXXX
Proceratium avium	CASENT0059014	XXXXXXXX	XXXXXXXX	XXXXXXXX	XXXXXXXX	XXXXXXXX	XXXXXXXX	XXXXXXXX	XXXXXXXX	XXXXXXXX	XXXXXXXX	XXXXXXXX
Proceratium SC02	CASENT0159684	XXXXXXXX	XXXXXXXX	XXXXXXXX	XXXXXXXX	XXXXXXXX	XXXXXXXX	XXXXXXXX	XXXXXXXX	XXXXXXXX	XXXXXXXX	XXXXXXXX
Proceratium silaceum	CASENT0235164	XXXXXXXX	XXXXXXXX	XXXXXXXX	XXXXXXXX	XXXXXXXX	XXXXXXXX	XXXXXXXX	XXXXXXXX	XXXXXXXX	XXXXXXXX	XXXXXXXX
Proceratium stictum	CASENT0106095	AY703557	AY703624	AY703691	AY703758	EF013497	KJ861146	KJ861757	KJ860486	KU671940	KU672017	KU671863
Promyopias silvestrii	CASENT0178751	XXXXXXXX	XXXXXXXX	XXXXXXXX	XXXXXXXX	XXXXXXXX	XXXXXXXX	XXXXXXXX	XXXXXXXX	XXXXXXXX	XXXXXXXX	XXXXXXXX
Protanilla JP01	CASENT0007002	EF013053	EF013761	EF013181	EF013633	EF013499	KU671663	KU671726	KU671789	KU671941	KU672018	KU671864
Protanilla TH01	CASENT0119776	XXXXXXXX	XXXXXXXX	XXXXXXXX	XXXXXXXX	XXXXXXXX	XXXXXXXX	XXXXXXXX	XXXXXXXX	XXXXXXXX	XXXXXXXX	XXXXXXXX
Protanilla TH02	CASENT0128922	XXXXXXXX	XXXXXXXX	XXXXXXXX	XXXXXXXX	XXXXXXXX	XXXXXXXX	XXXXXXXX	XXXXXXXX	XXXXXXXX	XXXXXXXX	XXXXXXXX
Protanilla TH03	CASENT0119791	XXXXXXXX	XXXXXXXX	XXXXXXXX	XXXXXXXX	XXXXXXXX	XXXXXXXX	XXXXXXXX	XXXXXXXX	XXXXXXXX	XXXXXXXX	XXXXXXXX
Protanilla VN01	CASENT0179564	XXXXXXXX	XXXXXXXX	XXXXXXXX	XXXXXXXX	XXXXXXXX	XXXXXXXX	XXXXXXXX	XXXXXXXX	XXXXXXXX	XXXXXXXX	XXXXXXXX
Protanilla VN03	CASENT0179565	XXXXXXXX	XXXXXXXX	XXXXXXXX	XXXXXXXX	XXXXXXXX	XXXXXXXX	XXXXXXXX	XXXXXXXX	XXXXXXXX	XXXXXXXX	XXXXXXXX
Psalidomyrmex procerus	CASENT0003082	EF013054	EF013762	EF013182	EF013634	EF013500	XXXXXXXX	XXXXXXXX	XXXXXXXX	XXXXXXXX	XXXXXXXX	XXXXXXXX
Pseudoponera stigma	CASENT0106311	XXXXXXXX	XXXXXXXX	XXXXXXXX	XXXXXXXX	XXXXXXXX	XXXXXXXX	XXXXXXXX	XXXXXXXX	XXXXXXXX	XXXXXXXX	XXXXXXXX
Rhytidoponera chalybaea	CASENT0106000	EF013058	EF013766	EF013186	EF013638	EF013505	FJ939885	KJ523705	KJ523622	KU671942	KU672019	KU671865
Simopelta pergandei cf	CASENT0052744	EF013061	EF013769	EF013189	EF013641	EF013508	XXXXXXXX	XXXXXXXX	XXXXXXXX	XXXXXXXX	XXXXXXXX	XXXXXXXX
Stenamma expolitum	CASENT0052774	KJ860019	KJ861907	KJ861294	KJ861478	KJ859831	GU085793	KJ861704	KJ860433	XXXXXXXX	XXXXXXXX	XXXXXXXX
Stigmatomma boltoni	CASENT0179570	KU671413	KU671566	KU672037	KU671515	KU671464	KU671623	KU671686	KU671749	KU671890	KU671967	KU671813
Stigmatomma denticulatum	CASENT0906827	KU671419	KU671572	KU672043	KU671521	KU671470	KU671629	KU671692	KU671755	KU671896	KU671973	KU671819
Stigmatomma mystriops	INB0003690672	KU671430	KU671583	KU672054	KU671532	KU671481	KU671640	KU671703	KU671766	KU671907	KU671984	KU671830
Stigmatomma pallipes	CASENT0106070	AY703554	AY703621	AY703688	AY703755	EF013381	KJ523366	KJ523716	KJ523633	KU671908	KU671985	KU671831
Stigmatomma saundersi	CASENT0006813	KU671432	KU671585	KU672056	KU671534	KU671483	KU671642	KU671705	KU671768	KU671910	KU671987	KU671833
Streblognathus peetersi	CASENT0260406	XXXXXXXX	XXXXXXXX	XXXXXXXX	XXXXXXXX	XXXXXXXX	XXXXXXXX	XXXXXXXX	XXXXXXXX	XXXXXXXX	XXXXXXXX	XXXXXXXX
Tatuidris tatusia	CASENT0423526	EF013067	EF013775	EF013195	EF013647	EF013516	KJ861147	KJ861758	KJ860487	KU671944	KU672021	KU671867
Tetraponera punctulata	CASENT0106098	AY703581	AY703648	AY703715	AY703782	EF013523	XXXXXXXX	XXXXXXXX	XXXXXXXX	XXXXXXXX	XXXXXXXX	XXXXXXXX
Tetraponera rufonigra	CASENT0106099	AY703582	AY703649	AY703716	AY703783	EF013524	FJ939892	KJ523718	KJ523635	XXXXXXXX	XXXXXXXX	XXXXXXXX
Thaumatomyrmex atrox	CASENT0010121	EF013074	EF013782	EF013202	EF013654	EF013525	XXXXXXXX	XXXXXXXX	XXXXXXXX	XXXXXXXX	XXXXXXXX	XXXXXXXX
Xymmer muticus	CASENT0006827	EF012960	EF013668	EF013088	EF013540	EF013380	KU671653	KU671716	KU671779	KU671921	KU671998	KU671844
Yavnella argamani	CASENT0235253	KU671449	KU671602	KU672073	KU671551	KU671500	KU671665	KU671728	KU671791	KU671945	KU672022	KU671868
Ampulex compressa	CASENT0217334	KU671444	KU671597	KU672068	KU671546	KU671495	KU671655	KU671718	KU671781	KU671923	KU672000	KU671846
Apis mellifera	CASENT0106100	AY703551	AY703618	AY703685	AY703752	EF013389	XXXXXXXX	XXXXXXXX	XXXXXXXX	XXXXXXXX	XXXXXXXX	XXXXXXXX
Aporus niger	CASENT0106104	EF012968	EF013676	EF013096	EF013548	EF013391	XXXXXXXX	XXXXXXXX	XXXXXXXX	XXXXXXXX	XXXXXXXX	XXXXXXXX
Apterogyna ZA01	CASENT0106304	KJ860058	KJ861946	KJ861333	KJ861517	KJ859870	KJ861143	KJ861754	KJ860483	KU671926	KU672003	KU671849
Brachycistis sp	CASENT0106122	EF012959	EF013667	EF013087	EF013539	EF013379	XXXXXXXX	XXXXXXXX	XXXXXXXX	XXXXXXXX	XXXXXXXX	XXXXXXXX
Chalybion californicum	CASENT0106103	EF012981	EF013689	EF013109	EF013561	EF013407	KU671657	KU671720	KU671783	KU671928	KU672005	KU671851
Chyphotes mellipes	CASENT0106101	AY703552	AY703619	AY703686	AY703753	EF013409	XXXXXXXX	XXXXXXXX	XXXXXXXX	XXXXXXXX	XXXXXXXX	XXXXXXXX
Dasymutilla aureola	CASENT0106123	EF012986	EF013694	EF013114	EF013566	EF013414	XXXXXXXX	XXXXXXXX	XXXXXXXX	XXXXXXXX	XXXXXXXX	XXXXXXXX
Metapolybia cingulata	CASENT0106106	EF013011	EF013719	EF013139	EF013591	EF013448	XXXXXXXX	XXXXXXXX	XXXXXXXX	XXXXXXXX	XXXXXXXX	XXXXXXXX
Mischocyttarus flavitarsis	CASENT0106102	AY703553	AY703620	AY703687	AY703754	EF013451	XXXXXXXX	XXXXXXXX	XXXXXXXX	XXXXXXXX	XXXXXXXX	XXXXXXXX
Pristocera MG01	CASENT0006958	EF013049	EF013757	EF013177	EF013629	EF013494	XXXXXXXX	XXXXXXXX	XXXXXXXX	XXXXXXXX	XXXXXXXX	XXXXXXXX
Sapyga pumila	CASENT0106105	EF013059	EF013767	EF013187	EF013639	EF013506	XXXXXXXX	XXXXXXXX	XXXXXXXX	XXXXXXXX	XXXXXXXX	XXXXXXXX
Scolia verticalis	CASENT0106107	EF013060	EF013768	EF013188	EF013640	EF013507	KU671664	KU671727	KU671790	KU671943	KU672020	KU671866